university of groningen / faculty of mathematics and natural sciences

Zernike Institute for Advanced Materials

Optical Condensed Matter Group (OCMP)

Optical studies of Ni and Cu Based Hybrid Materials

Master Thesis

by

Davood Abbaszadeh

Supervisor:

Prof. Dr. Paul van Loosdrecht

Referee:

Prof. Dr. Beatriz Noheda

July 21, 2011

Outline of the thesis

Inorganic-organic hybrids are a class of material that includes both organic and inorganic moieties at the same time. These materials have been studied extensively in view of their potential applications in different fields like, catalysis, gas separation and storage, as well as in view of their intriguing magnetic, optical, and electronic properties making them potentially suitable for data storage and processing applications. This large class of materials combines the advantages of organic and inorganic material in one substance. Organic materials are versatile and relatively easy and cheap to synthesize, whereas the inorganic materials have many interesting electronic properties which may be used in functional applications. Some of the general properties of in particular the Ni- and Cu-hybrid materials which are used in the research presented in this Master thesis will be discussed in chapter 1.

In this project, we have studied some of the physical properties of Ni and Cu based hybrid materials and we will discuss them in two parts. In the first part (chapter 2), we will focus on the dynamical properties of a one dimensional Ni-hybrid as seen by Raman spectroscopy. The second part (chapter 3) is devoted to the optical properties of a two dimensional Cu-Hybrid, in particular focusing on the birefringence experiments to study the polar phase transition found in this material just above room temperature.

Table of Contents

Chapter 1

1 An Introduction to Organic and Inorganic Hybrids

1.1 Classification of Organic-Inorganic Hybrids

Inorganic-organic hybrids are a class of material that includes both organic and inorganic moieties at the same time. These materials have been studied extensively in view of their potential applications in different fields like, catalysis, gas separation and storage, as well as in view of their intriguing magnetic, optical, and electronic properties making them potentially suitable for data storage and processing applications. This large class of materials combines the advantages of organic and inorganic material in one substance. Organic materials are versatile and relatively easy and cheap to synthesize, whereas the inorganic materials have many interesting electronic properties which may be used in functional applications. Nowadays, there is tremendous number of organic-inorganic hybrid materials known. So to avoid confusion arising from the complexity and diversity of these type materials; it could be very helpful to have a classification. Cheetham et al.[^{1}] have proposed a classification system based on connectivity of the inorganic and organic components inside the crystalline hybrid material. In this classification only covalent and ionic bonds are important and all others, such as hydrogen bonds and van de Waals bonds, are ignored. Table 1 shows this classification system. I and O are the symbol of inorganic and organic part of hybrid connectivity. So I^2 says that inorganic part has 2 dimensional connectivity and forms sheet like arrays. The O^n implies for

the metal-organic-metal connectivity. The classes of I^0O^0, I^1O^1, I^0O^2 and $I^{1-2}O^0$ are schematically represented in Figure 1. The square denotes the inorganic moiety and the circle the organic component. The black lines indicate an ionic or covalent interaction [**Error! Bookmark not defined.**].

In this study we focus on the I^1O^0 Ni-Hybrid and I^2O^0 Cu-Hybrid substances. Inorganic parts of these hybrids have one and two direct connection between them respectively. It allows strong magnetic interactions between them in the chain or sheet that they have arranged (1D inorganic chain and 2D sheet). Therefore, these materials with 1 and 2 inorganic dimensionality may show interesting physical properties that we are going to study some of them, lattice dynamics in Ni-Hybrid and polarization in Cu-Hybrid.

Table 1- Classification of inorganic–organic hybrid framework solids.

I^n: Inorganic connectivity

O^n: Metal-Organic-Metal connectivity	n = 0	1	2	3
0	I^0O^0 Molecular Complex	I^1O^0 Inorganic Network Hybrid	I^2O^0 Inorganic Network Hybrid	I^3O^0 Inorganic Network Hybrid
1	I^0O^1 Coordination Polymer	I^1O^1 Mixed Layers	I^2O^1 Mixed Framework	—
2	I^0O^2 Coordination Polymer	I^1O^2 Mixed Framework	—	—
3	I^0O^3 Coordination Polymer	—	—	—

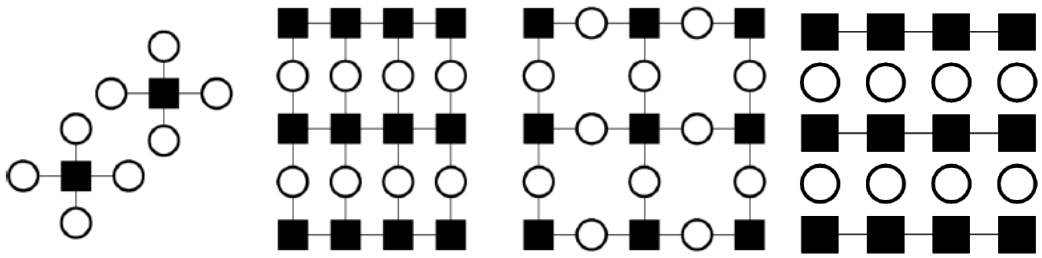

I^0O^0 **I^1O^1** **I^0O^2** **I^1O^0**

Figure 1- Schematic representation of three examples of organic-inorganic hybrids. The squares and the circles denote the inorganic and organic components respectively.

1.2 Crystal Structures

The crystal structure of the Mn, Fe, Co, Ni and Cu hybrids have been studied by Arkenbout et al. [1] by means of single crystal diffraction. Three types of crystal structures 0D, 1D and 2D

are presented in Figure 2. The Ni hybrid composition is $NiCl_3(C_6H_5CH_2CH_2NH_3)$ and it crystallizes into a 1D structure; the Cu-hybrid has composition $CuCl_4(C_6H_5CH_2CH_2NH_3)_2$ and crystallizes in a 2D structure. Inorganic $NiCl_6$ makes the back bone of the structure like a chain and is surrounded by organic parts with hydrogen bonds as showed in Figure 3 (left). In Cu-Hybrid $CuCl_4$ octahedrons makes buckled 2D structure that is shown in Figure 3 (Right). This Figure also shows that hydrogen atoms from ammonium ion have made hydrogen bonds with the chlorine atoms. As represented in the picture, for the Cu-hybrid 2 hydrogen bonds are stronger than the other one due to buckled structure of $CuCl_4$ octahedrons. In fact this is the origin of an electrical polarization in this material. Table 2 shows the crystallographic parameters that are related to the different magnetic hybrids with related space group as derived from the diffraction experiments.

Table 2- Crystal structures and crystal parameters of some hybrids, $MCl_{3+x}(C_6H_5CH_2CH_2NH_3)_{1+x}$ [**Error! Bookmark not defined.**]

	Mn	Fe	Co	Ni	Cu
Spacegroup	Pbca	Pbca	$P2_1/c$	$P2_12_12_1$	Pbca
a	7.1423(8)	7.0173(8)	7.277(2)	5.9055(6)	7.2099(9)
b	7.2306(8)	7.2466(8)	25.691(7)	6.8925(7)	7.2664(9)
c	39.121(4)	38.852(4)	11.110(3)	25.614(3)	38.238(5)
V	2020.3(4)	2001.0(4)	1996.1(10)	1042.58(19)	2003.3(4)
$wR(F^2)$	0.1124	0.1250	0.1264	0.0986	0.1120

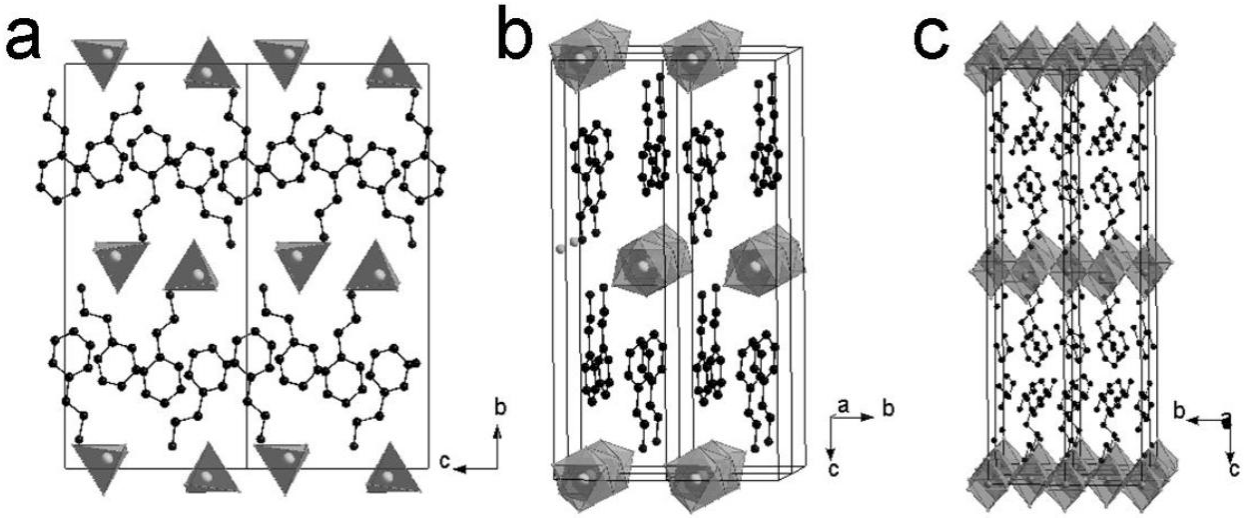

Figure 2 - The crystal structure of the nickel hybrid shows 1-dimensional inorganic arrays of face sharing NiCl6 octahedral [**Error! Bookmark not defined.**].

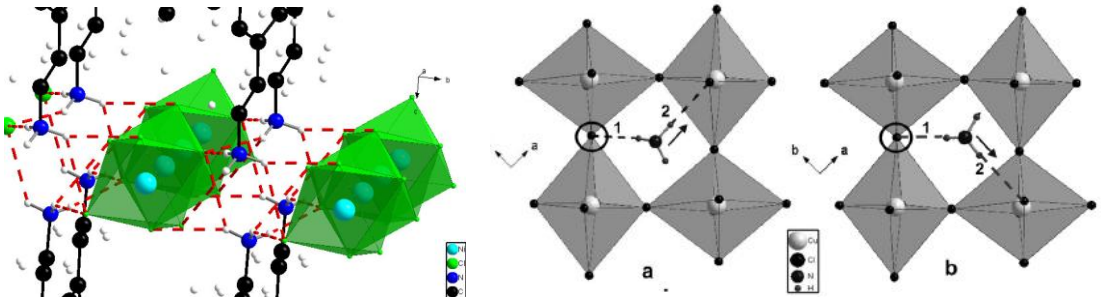

Figure 3-The hybrid is held together via the hydrogen bonds (shown as dotted lines) between the Cl atoms in the inorganic part and the hydrogens of the ammonium group in the organic part, **(left)** Ni-Hybrid, **(right)** Cu-Hybrid, in the latter case the CuCl octahedrons are distorted due to a Jahn-Teller Effect [**Error! Bookmark not defined.**].

1.3 Magnetic Ni-Based Organic-Inorganic Hybrid [I^1O^0]

In the following we will have a short review on magnetic properties of I^1O^0, Ni-hybrid. In this material, magnetic interaction occurs via super exchange. The source of magnetic dipole are the unpaired electrons on the 3d metal ions. There are two important criteria to make ordered magnetism, firstly the material should have magnetic dipoles and secondly the magnetic interaction should be sufficiently strong. The transition metals lie in the middle of the periodic table and they have an incomplete d-subshell in the neutral or ionic state (e.g. Ni=[Ar] $4s^1$ $3d^9$ and Ni^{2+}=[Ar] 4s $3d^8$). The d-orbitals are the outermost orbitals and crystal field has strong effect on them. These sub shell unpaired electrons have the key role in transition metals magnetic properties.

For example, the neutral Ni lies on top of group 10. Its ion in the hybrid compound is Ni^{2+}. Then the number of electron of d shell will be 8, and the level filling should be in accordance with the Hund's rules. This rule says that electrons like to fill each of those degenerate orbital with the same spin order. For 2 times ionized Ni this rule results 2 unpaired spin and total spin quantum number will be S=1. In Ni hybrid crystal, the Ni ion is surrounded by 6 inorganic ligands (Cl), that they will form octahedron around the Ni ion. It is obvious that these ligands will affect the energy levels in Ni, especially for the outer d orbital. In particular, this level will lose its degeneracy. In our case, octahedron, the split up is shown in Figure 4. As the figure shows two of levels shift up and the other three have some shift down in accordance with isolated ion. This splitting energy amount depends on the type of ligands. It should be noted that this splitting never changes the quantum number of spin in Ni^{2+} like to Mn^{2+} that causes ion come from high spin to low spin situation. Therefore octahedron distortion effect does not change magnetic moment of the Ni ion.

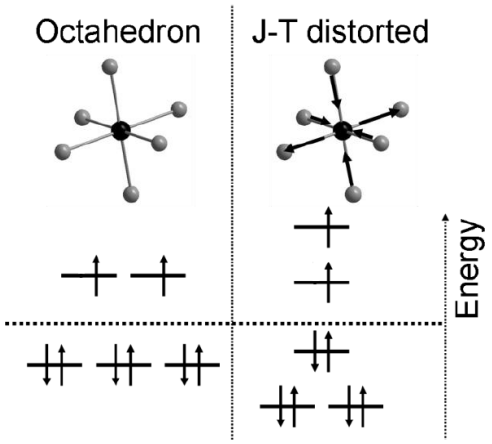

Figure 4 - A schematic representation of the d-orbital energies for the Ni^{2+} ion in an octahedral environment (left). Distortion due to Jan-Teller effect the quantum spin value will remain the same (right).

In addition to magnetic moment, an interaction that orders the moments is necessary. There are different interactions that have been discussed in magnetism books [e.g.[2]].

The most common interactions are dipole-dipole, direct exchange, RKKY, and superexchange. Generally the dipole-dipole interactions are very small between magnetic atoms, and ordering occurs below the 1K.

When the distance between two magnetic ions is enough close (less than 3A), their orbital can overlap and direct exchange between ions can occur. Orientation of orbitals relative to each other and the number of electrons in the outer orbitals determine the sign of interaction.

There are many different materials where magnetic ions in them are intermediated by a nonmagnetic ion. In this system magnetic interaction can occur via the intermediate ion, known as indirect exchange or superexchange. In Ni hybrid the magnetic interaction should be superexchange interaction, and the intermediating ion between two Ni ion is Chlorine ion.

RKKY interaction occurs in conducting material where the magnetic interaction can be mediated by the conduction electron [for more refer Blundell book]

Figure 5 shows schematically the electronic overlap of magnetic ion d orbital with chlorine p orbital. In superexchange interaction, its sign depends on the metal-ligand-metal angle and the number of electrons in the d-orbitals of each magnetic ion. For identical magnetic ions and an angle of 180°, the interaction will be antiferromagnetic.

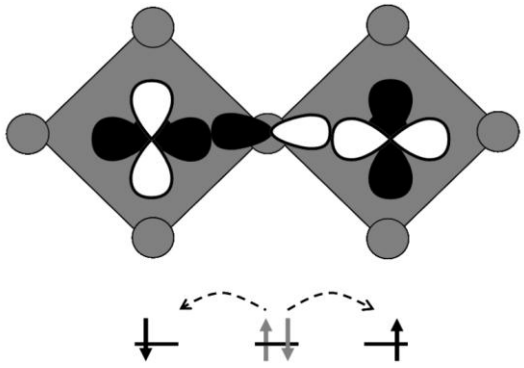

Figure 5-Middle ion is non-magnetic chlorine ion that plays intermediate ion role between magnetic ions in superexchange interaction. The magnetic d-orbital of the transition metal ions overlap with the p-orbital of the chlorine atom (the dumbbell in the middle). [**Error! Bookmark not defined.**].

1.4 Electrical Polarization in the Cu-Hybrids

In Cu-Hybrid, due to buckling of octahedrons, the ammonium group forms hydrogen bonds with one of in plane and one of out of plane chlorines as shown in Figure 6 (showed by circles). The third hydrogen bond of the ammonium group is weaker than the others. Arkenbout studies have revealed that hydrogen-bond (1) (Figure 6) is formed with an in-plane chlorine with the shortest bond length (2.321 A) and the favorable N-H-Cl angle (172.28°). But the second hydrogen-bond (2) is formed with an out-of-plane chlorine. This bond is weaker than hydrogen-bond (1) as the distance is larger 2.368 A and the angle is less ideal 168.69°. Now for the third hydrogen there are two chlorine atoms to make hydrogen bond. Due to buckling these two bonding don't have the same energy and they are not equivalent. Then the ammonium group feels two double potential wells that causes different shift of nitrogen atom. This shift can generate a local electric dipole depending on the bonding with in-plane and out of plane chlorine that is shown in figure 6c. Buckling of the structure, affects the magnitude and the orientation of the polarization.

It is expected that unpoled material be in a situation as Figure 6 shows. But by applied electric field it can shift to b situation and a net polarization can be produced.

Pyroelectric experiments have shown that cu-Hybrid is polar below 340K. Then it seems rational to measure the birefringence property of this material in order to observe the change of polarity under poling or phase transition with temperature. We will discuss the experiments in chapter 3.

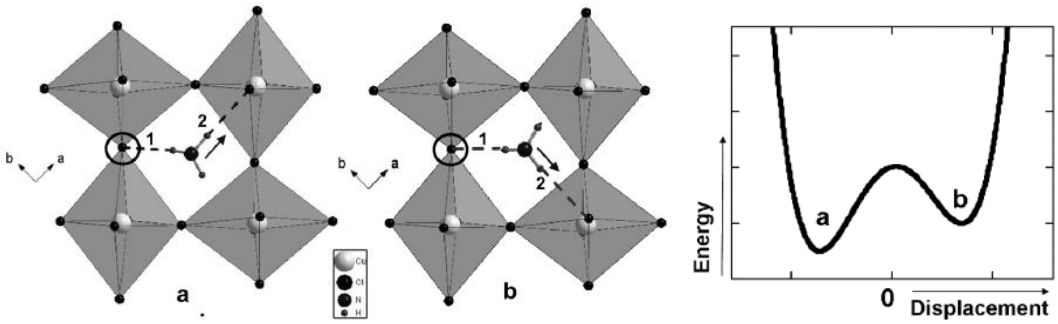

Figure 6- The ammonium group can occupy two different positions: a) and b) in the polar phase. Strongest hydrogen-bond (1) with the chlorine atom that is denoted with the circle. The second strongest hydrogen-bond (2) is formed between the ammonium group and an out-of-plane chlorine atom: for this bond the ammonium group has two options, a) and b). Both situations lead to an off-center shift of the nitrogen atom (denoted by the arrow), (c) energy diagram of the ammonium group with asymmetric double well potential [**Error! Bookmark not defined.**].

1.5 Synthesis Methods

Synthesis of hybrids is very easy. Procedure is mixing of two organic and inorganic solutions in stochiometric amounts and vaporizing the solvent. Crystallization process is in fact self assembly that is driven by the coulomb interactions and hydrogen bond that created between organic and inorganic part. Depending on the type of transition metal and organic part the self assembly results 0D, 1D or 2D inorganic arrays, which are interwoven with conjugated organic molecules. The general procedure to synthesis of magnetic hybrids has explained for different materials (Mn, Fe, Cu, Ni, Co) in Arkenbout PhD thesis. For Ni hybrid synthesis, ethanol is used as a solvent.

The crystals are grown by slow evaporation of the solvent in a stove at 62 °C with a $CaCl_2$ tube on the flask outlet, to prevent water from entering the system. Figure 7 shows the Ni hybrid crystal samples was made by this method.

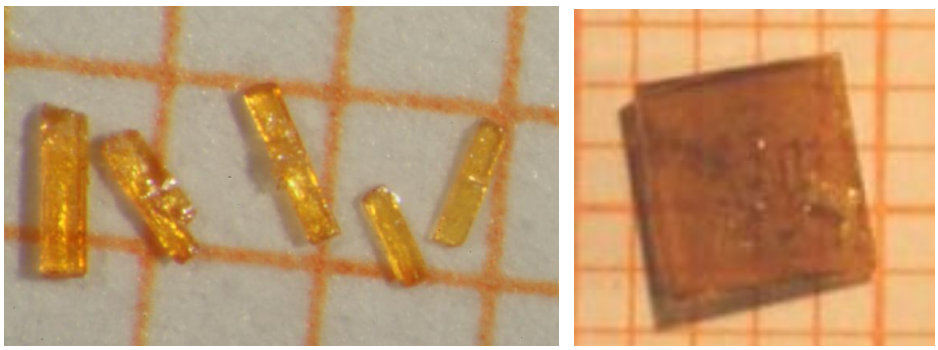

Figure 7: (Left) The crystals of the $NiCl_3(C_6H_5CH_2CH_2NH_3)$ hybrid, **(Right)** $CuCl_4(C_6H_5CH_2CH_2NH_3)_2$ crystals on mm paper [Arkenbout].

Chapter 2

2 Study of Ni-Hybrid by Raman Spectroscopy

2.1 Inroduction

In this chapter we will discuss the Raman Spectroscopy results from Ni-Hybrid. We have tried to observe the magnon observation and also we have studied the phase transition in the 1D Ni-Hybrid using Raman technique. At first we will review briefly the Raman Effect and then experiments will be discussed and this chapter will finish with conclusions about the Raman experiments.

2.2 Raman Effect

Raman Spectroscopy is one of the powerful techniques to study the different physical and chemical properties of materials in different fields such as pharmacy, polymer, semiconductors, thin films and nano-materials. It gives precious information about chemical and physical structure of the matter. In the following we will give a brief review of classic description of the Raman Effect.

2.3 Classical Description

In classical description, Raman Effect originates from the change of polarizability in molecules or in crystals due to existence of for instance vibrational modes. By applying an electric field, the polarizability of the system will change as a function of that field and it will produce a

dipole moment, $P_D=\alpha_0 E(\omega)$. If the applied field is electromagnetic plane wave with frequency of ω, and the system vibrates with a frequency of Ω, the polarizability will be modulated by the vibrational frequency as:

$$P_D(\omega) = (\alpha_0 + \alpha_1 \cos(\Omega t))E_0 \cos(\omega t) \quad (1)$$

Using trigonometric relations this leads to:

$$P_D(\omega) = \alpha_0 E_0 \cos(\omega t) + (\alpha_1 E_0 / 2)[\cos((\omega + \Omega)t)) + \cos((\omega - \Omega)t)] \quad (2)$$

Thus, the evanescing light oscillates not only with the frequency ω but also at sidebands with frequencies ω ±Ω. This means that outgoing light frequencies from material is not only in ω frequency but also it includes two other frequencies ω ±Ω (called Stokes and anti-Stokes). In general, α_1 is many orders of magnitude smaller than α_0, so the side bands are extremely weak in comparison with elastically scattered light. In crystals the situation is more complicated because they have periodic structures and atoms in this system vibrate in many ways and each could have its own specific energy and symmetry through the crystal lattice, these modes are called phonons.

If we consider the phonons as a particle so we can deal with the scattering as a inelastic collision of classical particles. The energy and momentum conservation (Figure 1) relations can be written as:

$$\begin{aligned} \hbar\omega_i &= \hbar\omega_s + \hbar\Omega \\ \hbar q_i &= \hbar k_s + \hbar q \end{aligned} \quad (3)$$

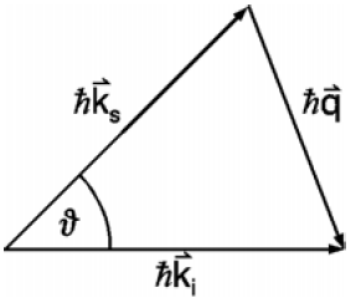

Figure 1 - Momentum conservation for a light-scattering process with phonon generation; ki, k_s, and q: wave vector for incident and scattered photon and for the phonon, respectively [3].

The sidebands are interpreted as emission or absorption of a phonon by the light with conservation of energy. The indices s and i refer to the scattered and incident light, respectively. The + sign is for phonon generation and – sign for absorption.

Intensity of sidebands is proportional to incident light intensity, so the ratio of scattered light to incident light will define scattering cross section as below:

$$\frac{d\sigma}{d\overline{\Omega}} = \frac{1}{I_i}\frac{d\Phi_s}{d\overline{\Omega}}$$ differential scattering cross section 4a

$$S = \frac{1}{V}\frac{d\sigma}{d\overline{\Omega}}$$ and Raman cross section 4b

Where $d\Phi_s$ is the light power (in watts) scattered into the solid angle $d\Omega$, I_i the intensity of the incident light (irradiance) in watts/m^2 and V the scattering volume. S is a cross section per unit volume and thus a property of the material [3].

To evaluate Raman Effect in crystals, it could be very helpful to use susceptibility tensor instead of scalar polarizability factor α. Also, to study crystal dynamics, normal Q_k of the oscillations are used to describe the displacements of atoms in crystal. If we expand the susceptibility with respect to the normal coordinates Q_k we can obtain:

$$\chi_{jl} = (\chi_{jl})_0 + \sum_k \left(\frac{\partial \chi_{jl}}{\partial Q_k}\right)_0 Q_k + \sum_{k,m}\left(\frac{\partial^2 \chi_{jl}}{\partial Q_k \partial Q_m}\right)_0 Q_k Q_m + \ldots \quad 5$$

In the second term, $\partial\chi_{jl}/\partial Q_k = (\chi_{jl})_k$, gives the component of Raman tensor for any normal coordinates or displacements in specified normal coordinates. In crystal the intensity of Raman scattered light is proportional to the square of the Raman tensor. For any mode, this matrix is 3×3 matrix determined from derived susceptibilities. The induced dipole that is responsible for the emission of sidebands, with an incident light $E^i_l(t) = E^i_0\cos(\omega t)$ and phonon – $Q_k = Q_{k0}\cos(\Omega_k t)$ – and by considering of first order approximation of susceptibility (linear approximation)- $\chi_{jl} = (\chi_{jl})_0 + (\chi_{jl,k})_0 Q_k$ - will be:

$$P_D(\omega \pm \Omega_k) = \chi_{jl,k}\varepsilon_0 V_u E^i_{l0} Q_{k0}\cos((\omega \pm \Omega_k)t)) \quad 6$$

Where V_u is the volume of the unit cell. In Raman Scattering the geometry of the direction of incident and scattered light and also directions of polarizations are important. To describe the geometry of scattering, it is convenient to use Proto Notation that its form is a(bc)d, in which a and d denotes the coming and outgoing light wave vector directions, b and c show the directions of the coming and outgoing light polarization (Electric Field) respectively.

Regarding to the geometry of scattering, for a selected direction of polarization (e^s) of the scattered light, scattering intensity is proportional the absolute square of the projection of the P^s_D on e^s.

$$\Phi(k) = C\left|e^s P^s_D\right|^2 = C\left|\sum_j e^s_j P^s_{Dj}(k)\right|^2 \quad 7$$

where P^s_{Dj} are the components of the dipole moment induced by the Raman effect. This dipole moment is given according to 6

$$P^s_{Dj} = \sum_l \chi_{jl,k} e^i_l E_0 V_u \varepsilon_0 Q_k \qquad 8$$

e^i_l are the of the unit vector of polarization for the coming light. By replacing this in equation 7, one can find the intensity of scattered light as:

$$\Phi(k) = C\left|e^s(\chi_k e^i)\right|^2 = C\left|\sum_j e^s_j \chi_{jl,k} e^i_l\right|^2 E_0{}^2 \qquad 9$$

This equation shows the possibility of measuring of Raman scattering intensity for any Raman tensor component by selecting the proper combination of the incoming and scattered polarization. Here we are not going to enter the quantum mechanical description of the Raman effect. But it noteworthy to mention that according to selection rules of Raman, the modulation of the lattice can be shown as Figure 2. It shows that by excitation of vibrational states 2 options for relaxation can be expected. As it depicted in the Figure 2 if the modulated wavelength energy is less than excitation energy, the scattering are called Stokes scattering, in the reverse case it is called anti-Stokes Raman scattering [For more refer to 3].

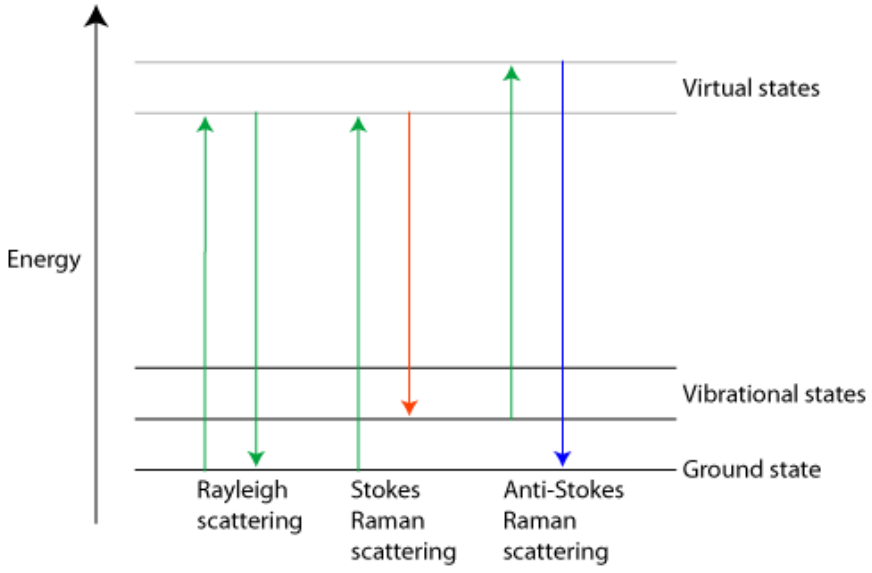

Figure 2- Schematically representation of Raman Effect process.

2.4 Magnetic Order in the 1-dimensional Hybrid

As it mentioned already Ni- hybrid is 1 dimensional inorganic chain. This hybrid has three distinct regions: 1- the paramagnetic, 2- the short rang order and 3- the long range order regime. As is shown in last section, the paramagnetic phase confirms the S=1 state of the Ni^{2+} and also the Weiss constant is negative, -71 K, that indicates antiferromagnetic interaction.

The long range magnetic order is suppressed in the 1-dimensional [**Error! Bookmark not defined.**]

According to Arkenbout studies, the notable effect about Ni-hybrid, is its susceptibility behavior at low temperature – around 8K. This behavior is different than 1D antiferromagnetic that is expected. This deviation firstly suspected that is because of opening of a Haldane gap. Haldane gap happens for systems that their spin is 1 and when the system undergoes the pairing of the spins it will cause a nonmagnetic ground state. The other guess is that this behavior could be due to existence of paramagnetic material. Many experiments of magnetization measurement on single crystal (below 8K in two different axis - along and perpendicular to chain) were done and is shown in Figure 3. Arknbout has discussed this anisotropy is the signature of long range order and presence of paramagnetic impurities. And Haldane gap cannot explain it, because these effect are isotropic. This anisotropy and T-dependence of magnetic susceptibility is similar to $RbNiCl_3$ compound [[4], [5]] which consist of similar 1D arrays of face sharing $NiCl_6$ octahedral. This similarity can be considered as a confirmation of presence of magnetically ordered state around 8K.

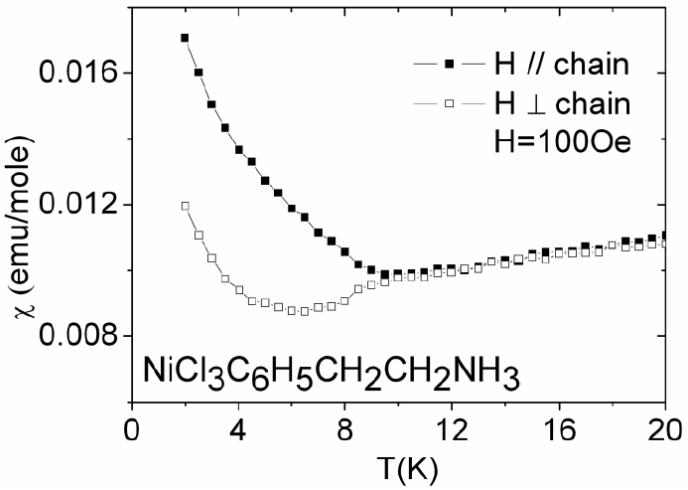

Figure 3- Magnetic susceptibility versus temperature in different crystallographic directions for the Ni-hybrid. Below 8 K anisotropy is observed, which indicates long range magnetic ordering [**Error! Bookmark not defined.**].

In the next section we will review our experiments about Ni-Hybrid. The purpose of the study was to observe the magnons and magnetic phase transitions. In addition to we investigated its phase transition at high temperature by comparing changes in Raman signature in different temperatures.

2.5 Experiments

Raman technique is one of the powerful techniques to observe the magnon quasi particles. We have performed polarization sensitive Raman spectra at different configuration and

temperatures. According to the Figure 3, we expected to observe the magnon scattering below 8K. Unfortunately the experiments results were not successful to observe magnon scattering at low temperature (below 8K). As we will see there was no appreciable difference in Raman spectra going from low to high temperatures to be attributed to magnon scattering (Figures 4 and 5). We measured Raman spectra at every 0.5K starting from 4K, but there was not observable change of spectra from 4 to 10K even 80K (changes like disappearing energy modes or sudden shift in modes place or intensity). It may the intensity of scattering is lower than we can observe via our set-up as it mentioned for the similar compounds [6]. Now, in the following the derived spectra from Ni-Hybrid at low temperature up to 320K will be discussed.

Raman is able to determine the structural phase transition under different physical conditions. Here we explored structural phase transition of Ni-Hybrid according to temperature using Raman technique. To do this we need to monitor the modes evolution in different temperatures. In all configurations list of the observed vibrational modes with respect to their energies are listed in the Appendix A.

Ni hybrid belongs to P 21 21 21, space group in group theory. This theory predicts 4 irreproducible representation, A_g, B_{1g}, B_{2g}, B_{3g}. In the c(aa)-c and c(bb)-c configuration only A_g mode should be observable. And in the c(ab)-c configuration B_{1g}. These mode tensors can be written as:

$$A_{1g} = \begin{pmatrix} a & 0 & 0 \\ 0 & b & 0 \\ 0 & 0 & c \end{pmatrix}, \qquad B_{1g} = \begin{pmatrix} 0 & d & 0 \\ d & 0 & 0 \\ 0 & 0 & 0 \end{pmatrix}, \quad B_{2g} = \begin{pmatrix} 0 & 0 & e \\ 0 & 0 & 0 \\ e & 0 & 0 \end{pmatrix}, \quad B_{3g} = \begin{pmatrix} 0 & 0 & 0 \\ 0 & 0 & f \\ 0 & f & 0 \end{pmatrix}$$

By considering these tensors one can understand that the spectrum in c(aa)-c and c(bb)-c configurations should be similar. Figure 4 shows the Raman spectra for Ni hybrid from 4K to 320K. Comparing the spectra in the two configurations reveals that they are mostly identical, except for the 209 and 272 cm^{-1} modes. Both configurations show a very strong mode at 119cm^{-1}. Modes with the wavenumber of 119, 209 and 272 cm^{-1} are assigned to A_g symmetry. These modes exist also in the other configurations that it could be because of leakage of polarization. This leakage comes from the alignment of sample relative to the polarization of light. Based on this reason the 161 and 167 cm^{-1} is assigned to B_{1g} mode, because these energies have very high intensity in B_{1g} mode in comparison to other configuration that the intensities are at least 6 times smaller. According the list of modes (listed in Appendix A), the following phonon modes are related to B_{1g} tensor; 90.7, 121, 126,

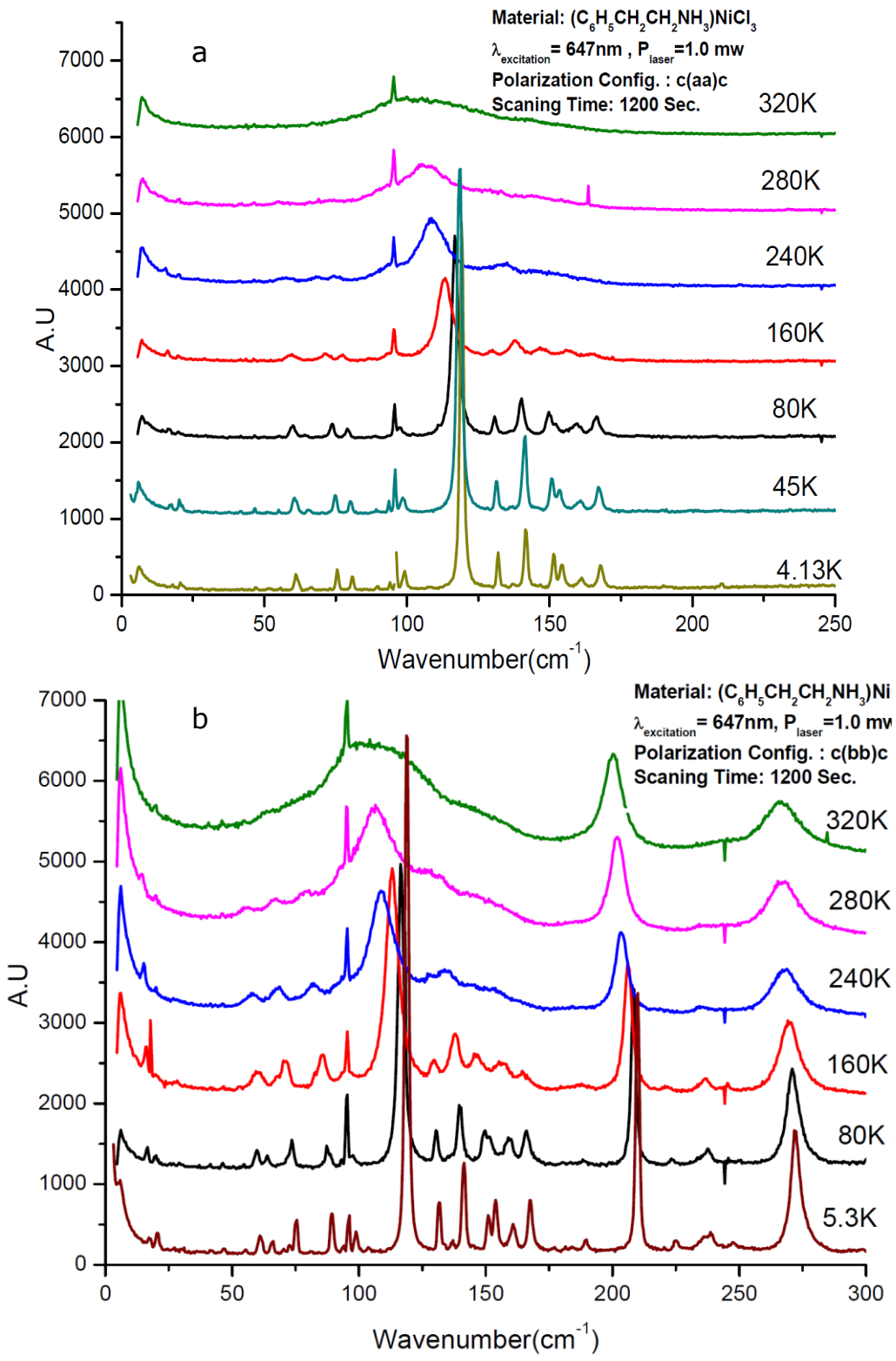

Figure 4- Raman Scattering of Ni hybrid in different temperature for c(aa)-c and c(bb)-c configurations.

133.4, 137, 144, 150.2, 176.1, 181cm^{-1}. The remaining modes are attributed to two other configurations.

The main differences that were observable at the first glance from the results were broadening and red shift of the modes that was observed for all configurations (Figure 4 and 5). We observed three main differences by increasing temperature in Raman signature in c(ab)-c configuration spectra. The first peculiar behavior belongs to B_{1g} configuration 168cm^{-1} mode that is very strong at low temperature and decreases in intensity rapidly and vanishes around 280K in which is shown in Figure 5. The second is the fixing of main mode (is shown by red vertical line in Figure 5b) around 149 cm^{-1} without shifting to the left. At the same time we observe the mode with energy 61cm^{-1} has considerable shift at 320K according to 280K at Figure 6a (the strongest mode was fixed in these two temperatures, Figure 5b). The energy mode 61cm^{-1} is related to the liberation mode or disorder orientation of organic part. It most probably is due to change of polarization status. In other words, Ni-Hybrid has a phase transition from polar structure to non-polar one. Similar effect was observed for Cu-Hybrid by Toni in our group.

These observed phenomenon suggest that Ni-Hybrid has a phase transition between 280 and 320K. In Figure 6a the position of the peaks is shown roughly but by fitting and analyzing our spectra we derived results of Figure 6b and 6c. It shows the Raman shift from low temperature to 280K is monotonically decreasing but it shows a sudden decrease after 280K. FWHM plot confirms that this mode broadens considerably after 280K (Figure 6c). Therefore we can say that Ni-Hybrid shows structural phase transition in between 280-300K.

To verify this claim, and also the structure, after phase transition X-Ray crystallography is needed. But according to the vanishing and shifting the liberation mode (61 cm^{-1}) we guess the chains change in a way that there is equal opportunity with equal bonding strength for ammonium ion hydrogens to make hydrogen bonding. And it will be possible if the 1D structure can get rid of structural distortion. According to Figure 3 in chapter 1 it is possible to make these bonds with 2 chlorine atoms from one wire and the next one with neighbor octahedral.

Looking in articles that they have studied Raman scattering of Nickel Chloride and the compositions that are included Nickel and Chlorine [6,7], they concluded that the 1D structure of $RbNiCl_3$ and also $NiCl_2$ don't show one or two magnon scattering, if such a scattering occurs, their intensity must be less than $1/30^{th}$ of the A_{1g} phonon. Comparing their results with Figure 4 it can be guessed that the vibrational mode at 210cm^{-1} and 272cm^{-1} are related to Ni-Cl vibration. Energy shift of vibrational modes in Figure 5 for all modes is shown. This graph also shows that two mentioned modes have the less energy shift relative to other modes. It could be due to ionic strong bonding between these elements. Because the chlorine has high electron affinity and will make stronger bonds with metals. Therefore their Raman scattering is

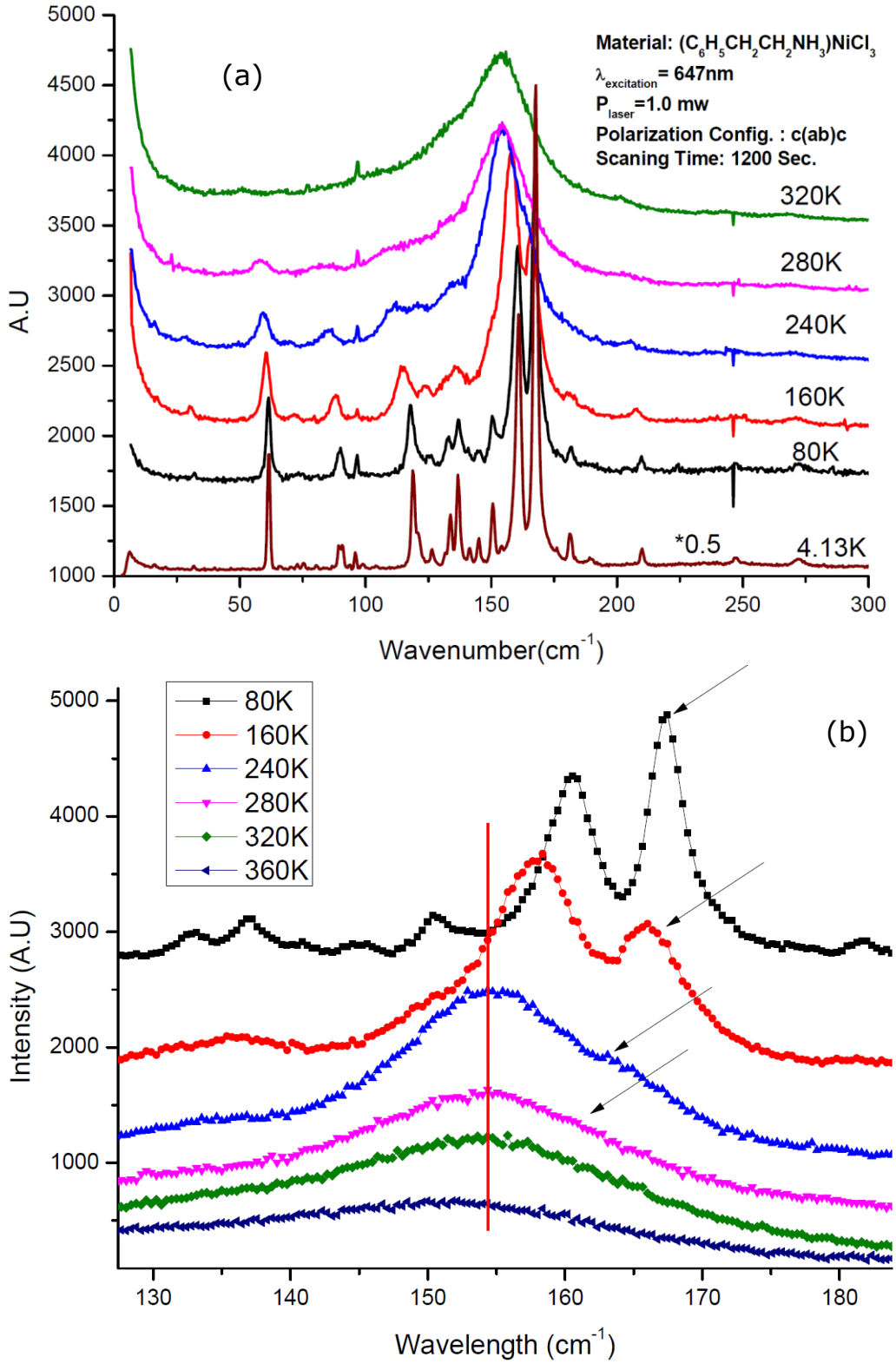

Figure 5- Raman Scattering of Ni hybrid in different temperature for different configuration, fitting and analyzing shows that mentioned peak vanishes after 280K (Appendix A2).

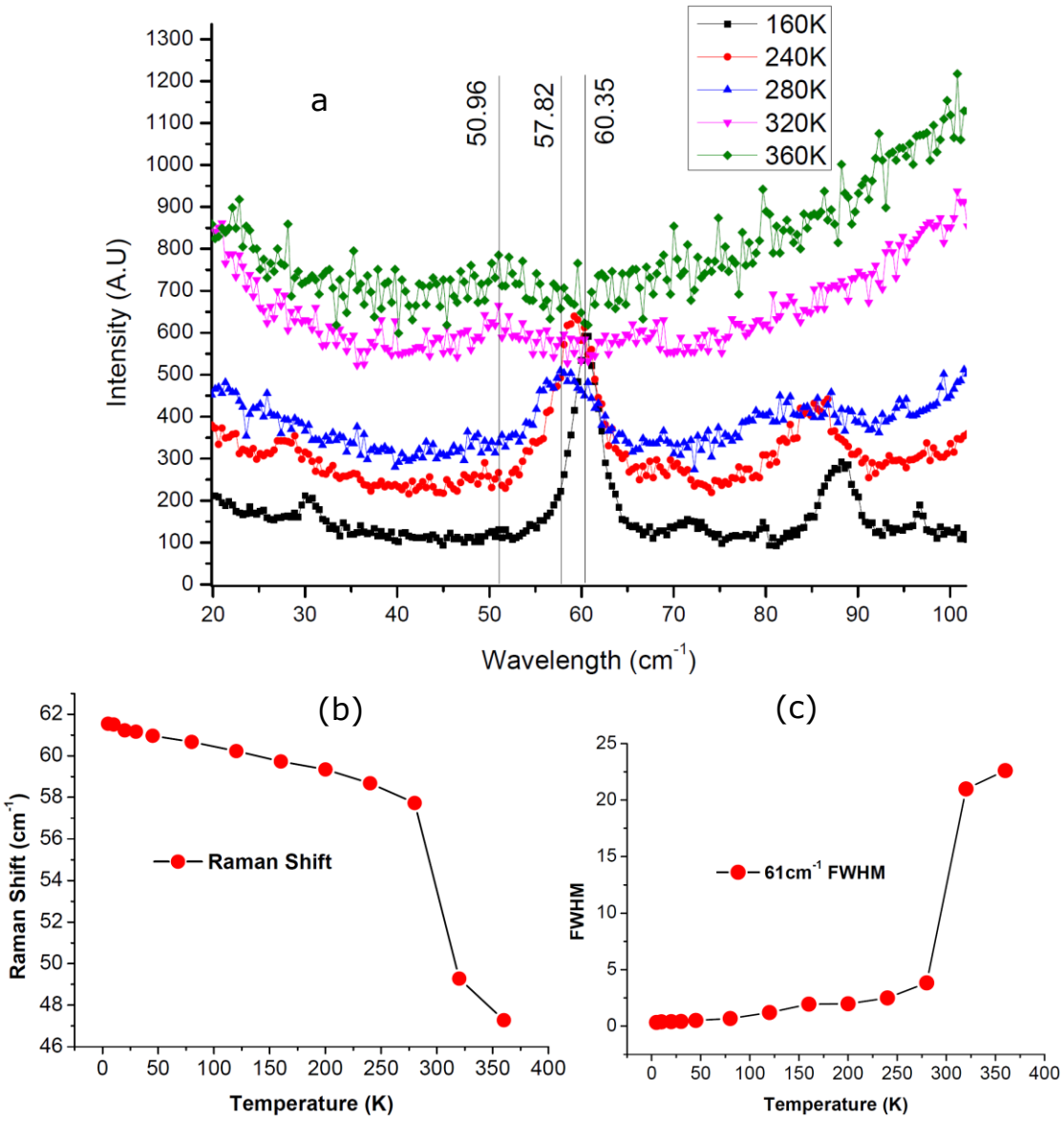

Figure 6- Shift of mode with energy ~60cm^{-1} that is 3 cm^{-1} from 160-280K, but it shows a considerable Raman shift (nearly 7 cm^{-1}) and stays in fixed energy above 320K.

enough strong to be observable still in high temperature that thermal randomly vibrations cannot overcome and cover them like other modes.

2.6 Conclusion

Our raman experiments on the Ni-hybrid ($NiCl_3(C_6H_5CH_2CH_2NH_3)$) did not reveal any magnon related scattering processes. Most likely the efficiency of any magnon scattering in this material is too low to be observable. From this sense, this work is in agreement with other research work that is about different 1D-Ni compounds like $NiCl_2$ and $RbNiCl_3$ [6,7].

We did observe that the Ni-Hybrid shows a phase transition around 300K. We found that a liberation mode (is related to organic inorganic bonding) shifts suddenly to low energy values and broadens considerably at the same time. We attribute this behavior to change of polar state in the Ni-hybrid in comparison to our group work on Cu-Hybrid. Cu-Hybrid shows this phase transition at 340K.

To verify the how the structure changes, x-ray crystallography is needed to do in both lower and higher 300K. But roughly can be guessed that the structure changes in a way that provides equal hydrogen bonding strength for all ammonium ion Hydrogens. And it will be possible if the 1D structure can get rid of structural distortion.

Chapter 3

3 Birefringent study of Cu-Hybrid

3.1 Birefringence

If we assume that atoms in crystalline lattice are connected to each other with well defined axes, optical properties of the lattice will be different along different crystalline axes; because, the atomic distances are not the same in all crystal axes. Difference in atomic distances in crystalline axes will cause the difference in vibrational frequencies (because electrons are anisotropic), and then refractive index will be different in different axes. Materials that have different crystal axes are called anisotropic crystals due to their optical anisotropy. This anisotropy gives rise to double refraction or birefringence behavior in the crystals. Birefringent property can be described by relationship between polarization, P, and applied electric field, E,

$$P = \varepsilon_{\circ} \chi E \qquad 1$$

where X is the susceptibility tensor. By choosing the right coordinates corresponds to the crystalline axes, susceptibility tensor can be written as below,

$$\chi = \begin{pmatrix} \chi_{11} & 0 & 0 \\ 0 & \chi_{22} & 0 \\ 0 & 0 & \chi_{33} \end{pmatrix} \qquad 2$$

In cubic crystalline structure, all 3 crystalline axes are same, therefore all of susceptibility tensor components are equal and crystal will have isotropic optical properties. Crystals like

hexagonal structure have 2 equal and one different axes. Then the optical properties will be same along equal a and b axes and different in c direction. This kind of crystals is called uniaxial crystals, this means $X_{11}=X_{22}$ and not equal with X_{33}.

Birefringence also is known as double refraction due to the decomposition of light into two beams when passes through the anisotropic object. Figure 1 schematically shows the splitting of two rays that passes through anisotropic crystal. Birefringence can be defined and derived by considering the dielectric permittivity and a refractive index that are tensors [8].

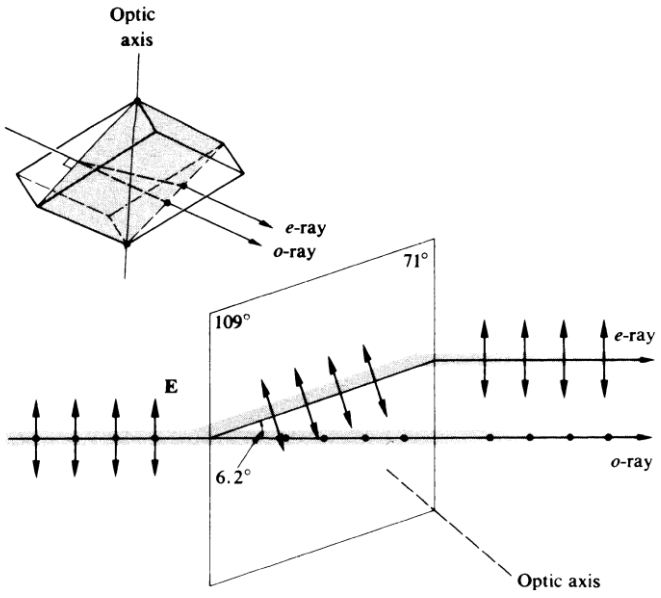

Figure 1- Unpolarized Light beam splits in to two orthogonal field components traversing a well known birefringent material Calcite due to difference in refractive index in different crystal axes ($n_{||}=1.486$ and $n_{\perp}=1.658$) [9]

Linear Dichroism (LD) is a phenomenon of anisotropic optical absorption, which means that one component of polarization of light, is more strongly absorbed than the other [10]. Circular Dichroism (CD) refers to the differential absorption of left and right circularly polarized light. This phenomenon is exhibited in the absorption bands of optically active chiral molecules.

3.2 Principle of measurement

If we place a dielectric material between two linear polarizers, then we will be able to examine that is it isotropic or anisotropic? When a polarized light goes through the anisotropic medium, it will experience two different refraction indices. These two rays have mutually orthogonal polarizations, that is named as the ordinary and extra ordinary rays as shown in Figure 1. These two rays due to experiencing different refractive indices, leading to a phase difference between the two beams of

$$\Delta = \frac{2\pi d(n_1 - n_2)}{\lambda} \qquad 3$$

where d is the thickness of the sample and λ is the wavelength of light. (n_1-n_2) is the birefringence of the sample or difference of the refractive index in different crystalline axes.

Figure 2 shows our experimental set-up schematically that is mostly similar to the standard methods that are proposed by different researchers. This set up includes some optical elements. These elements are:

White light source: that it produces light spectrum from 300-1000nm,
Monochromator: to filter single wavelengths from 300-1000nm range,
Focal lenses: that is used to keep the light in line thorough the set up,
Chopper: to modulate the transmitted light,
Polarizers: to polarize the light in certain direction,
Photoelastic modulator (PEM): to produce different kind of polarizations,
Detector: to detect the light that comes in different frequencies (in PEM oscillation and chopper rotation frequencies)

To consider this set up quantitatively, we have to use Jones matrices and evaluate the set up.

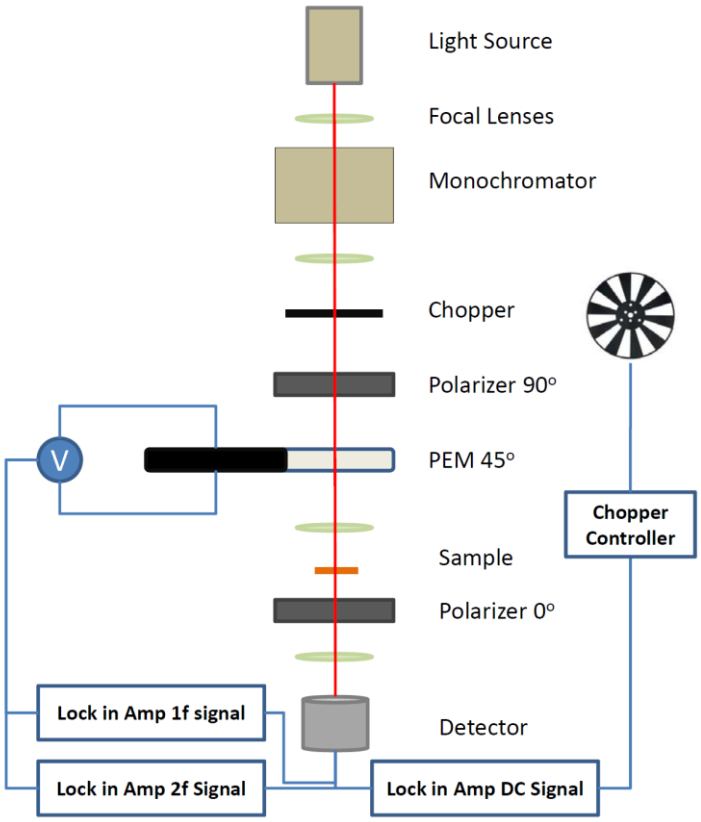

Figure 2 - Schematic birefringent measurement set up

3.2.1 Jones Calculus

The polarized light and optical objects can be described using Jones calculus. Polarizers and Retarders are such optical devices. Polarizers can covert non-polarized light to linearly or right and left circularly polarized light. Phase retarders introduce a phase shift between the vertical and horizontal component of the field and thus change the polarization of the beam. When light passes through different optical elements, the emerging light polarization and intensity can be calculated and evaluated by product of all Jones matrices related to the objects.

The Jones vector that shows the light polarization, can be written in the form of the components of plane wave as below

$$\begin{pmatrix} E_x(t) \\ E_y(t) \end{pmatrix} = \begin{pmatrix} E_{0x}e^{i(kz-\omega t+\varphi_x)} \\ E_{0y}e^{i(kz-\omega t+\varphi_y)} \end{pmatrix} = e^{i(kz-\omega t)} \begin{pmatrix} E_{0x}e^{i\varphi_x} \\ E_{0y}e^{i\varphi_y} \end{pmatrix} \quad 4$$

Here the vector without time and z dependence is the Jones vector. Jones vector includes the amplitude and the phase of electric field in two x and y directions. To simplify the calculation process we can normalize the vectors to 1.

Now we are going to compute the effect of one or a series of linear optical element on the polarized light that it can be linear or circular [10]. Optical elements are described using 2 x 2 matrices that are called Jones matrices. To see the effect of optical element, its matrix multiplied by polarized light vector. If we arrange a set of elements that light passes through, then the result is given by multiplication of elements matrices:

$$\begin{pmatrix} a_n & b_n \\ c_n & d_n \end{pmatrix} \cdots \begin{pmatrix} a_2 & b_2 \\ c_2 & d_2 \end{pmatrix} \begin{pmatrix} a_1 & b_1 \\ c_1 & d_1 \end{pmatrix} \begin{pmatrix} A \\ B \end{pmatrix} = \begin{pmatrix} A' \\ B' \end{pmatrix} \quad 5$$

3.2.2 Description of Experimental Set-up

Using the proper matrix of each element [11], we can describe our system according to equation 5 as below according the set-up in Figure 2:

$$\begin{pmatrix} E_{xf} \\ E_{yf} \end{pmatrix} = \begin{pmatrix} 1 & 0 \\ 0 & 0 \end{pmatrix} R(-\theta) \begin{pmatrix} ae^{i\varphi_1} & 0 \\ 0 & be^{i\varphi_2} \end{pmatrix} R(\theta) R\left(-\frac{\pi}{4}\right) \begin{pmatrix} e^{i\delta(t)} & 0 \\ 0 & 1 \end{pmatrix} R\left(\frac{\pi}{4}\right) \begin{pmatrix} 0 & 0 \\ 0 & 1 \end{pmatrix} \begin{pmatrix} E_{xi} \\ E_{yi} \end{pmatrix} \quad 6$$

where the first matrix is related to polarizer, R(θ) is the rotation matrix, the third matrix described the unknown sample (that is assumed is dichroic (a and b absorption coefficients 0<a,b<1) and birefringent (phase difference) at the same time. The matrix 6th from left describes the PEM. δ(t) is the phase that is changing sinusoidal by PEM and produces all kinds of polarizations by changing the time. The next matrix is analyzer that its polarization is perpendicular to the first polarizer. Finally the vector is the light coming from monochromator.

We derived the final equations as below that we will use to evaluate the birefringence of the hybrid crystals. By definition of K value that is a function of a and b parameters we can

evaluate the dichroic behavior of the samples. Because it depends to absorption factors of the crystal in different directions

$$K = \frac{2ab}{(a^2 + b^2)} \quad if \quad a = b \ then \quad K = 1 \qquad 7$$

The ratio of PEM modulated signals (V_{1f} and V_{2f} that are the modulated coming light signals that is measured for PEM oscillation frequency and its double frequency) to transmission signal intensity are needed to calculate the birefringence phase changes. Since the V_{1f} and V_{2f} are AC signals then we measure just root mean squared of them:

$$\frac{V_{1f,rms}}{V_{DC}} = \sqrt{2}K \sin(\Delta) J_1(A) \qquad 8$$

$$\frac{V_{2f,rms}}{V_{DC}} = \sqrt{2}K \cos(\Delta) J_2(A) \qquad 9$$

Equations 7, 8 and 9 enables us to calculate the phase difference and at the end birefringence vale as below:

$$\Delta = \arctan\left(\frac{J_2(A)}{J_1(A)} \times \frac{V_{1f,rms}}{V_{2f,rms}}\right) \Rightarrow n_1 - n_2 = \frac{\lambda}{2\pi d}\left\{\arctan\left(\frac{J_2(A)}{J_1(A)} \times \frac{V_{1f,rms}}{V_{2f,rms}}\right)\right\} \qquad 10$$

In the cases that crystal is non-dichroic, a and b coefficients are equal, K coefficient in equation will be 1, and one can calculate birefringence just by measuring V_{1f} and V_{DC} (Equation 8).

According to definition of dichroism, a and b that are the absorption coefficients in different direction of uniaxial crystal, linear dichroism can be defined as the a/b. K value from equation 7 can't give us the a/b, but we can use it to explain that the crystal is dichroic or not, if we know the birefringent value from equation 10.

To derive a/b ratio, there is different strategies. First one can remove the analyzer (second polarizer close to detector) in the set-up and rotate the sample parallel to first polarizer (close to light source) (Figure 2). Jones calculation can be done as below for this system,

$$\begin{pmatrix} E_{xf} \\ E_{yf} \end{pmatrix} = \begin{pmatrix} ae^{i\Delta} & 0 \\ 0 & b \end{pmatrix} R\left(-\frac{\pi}{4}\right) \begin{pmatrix} e^{i\delta(t)} & 0 \\ 0 & 1 \end{pmatrix} R\left(\frac{\pi}{4}\right) \begin{pmatrix} 0 & 0 \\ 0 & 1 \end{pmatrix} \begin{pmatrix} E_{xi} \\ E_{yi} \end{pmatrix} = \frac{1}{2} \begin{pmatrix} ae^{i\Delta}(e^{i\delta(t)} - 1) \\ b(e^{i\delta(t)} + 1) \end{pmatrix} \qquad 18$$

Detailed calculation is done in the appendix. In the end the ratio of V2f to VDC will give the dichroism a/b ratio,

$$LD \propto \frac{V_{2f}}{V_{DC}} = 2\sqrt{2} J_2(A) \frac{b^2 - a^2}{b^2 + a^2} \qquad 19$$

In this case one can also measure the circular dichroism, which is found as

$$CD \propto \frac{V_{1f}}{V_{DC}} \qquad 20$$

For detailed calculation refer to Appendix B2.

3.3 Experiments

3.3.1 Transmission Spectroscopy

When light strikes to an object, depending on its wavelength can be absorbed, reflected or transmitted. If the object absorbs the light, it converts the electromagnetic energy or heat. If we shine different wavelengths of lights, it selectively absorbs, reflects, or transmits certain wavelengths.

If we assume atoms or molecules are attached to each other by springs, their electrons according to the nature of atoms and crystal structure have a tendency to vibrate at a frequency that we say natural frequency. When a photon (with specific wavelength) strikes to an atom, it will induce vibrational motion to atom's electrons. Depending on the wavelength of the light that interacts with crystal, different scenarios will occur. If the frequency of the light equals the frequency of an electronic excitation, the light will be absorbed and converted to heat. Different materials have different absorption spectra, because each particular material has unique structure and composed of specific atoms. Therefore, their electrons will have different natural vibration frequencies than other materials.

If the frequency of light don't match the natural frequency of vibrating electrons, that light will be reflected or transmitted. In this case if the vibrations of the atoms are passed on neighbor atoms and reemit the light on the opposite side, matter is transparent. If the vibrations don't pass though the bulk, then it will be reemitted from surface atoms that mean the light is reflected.

In this project we investigate Cu-Hybrid ($CuCl_4(C_6H_5CH_2CH_2NH_3)_2$) by measuring its transmission, birefringence regarding to different wavelengths and temperatures. Figure 1 shows the transmission of the compound in different temperatures. These spectra are not normalized to light source spectrum, but it shows that material absorbs the nearly all the light below 500nm and above 750nm. Below 500nm p-d orbital transitions (that light is absorbed and then decays as heat and light in lower frequancies) and the light below 500nm is absorbed by material. This sample thickness is 205μm, but thinner samples show transmission higher than 800nm. Figure 2 shows normalized true transmission, for examples with different thickness, and we see there is some transmission above 800nm. This transmission is due to d-d transition in the material. Electron transitions in d orbitals are forbidden for full symmetric materials due to selection rules. But our material is not so symmetric anymore due to Jahn-

Teller effect and symmetric system selection rules does not apply for that. This is why we see some transmission of light higher than 800nm wavelengths.

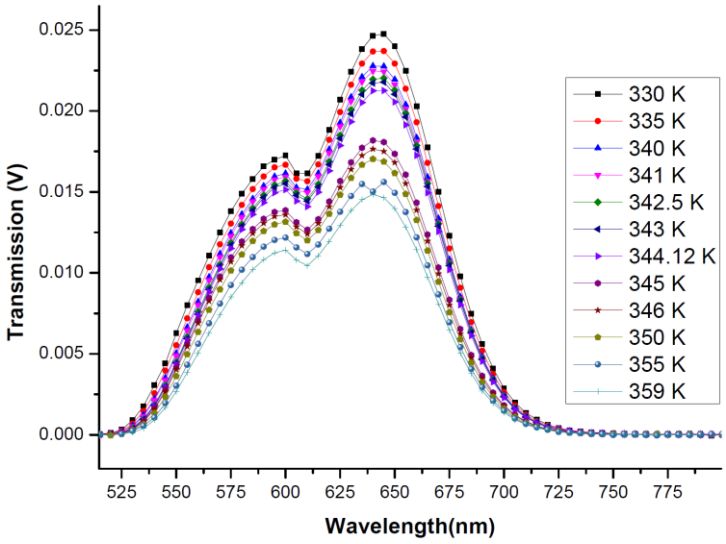

Figure 1 -Transmittance of light from Cu-Hybrid vs Wavelength in different temperatures (thickness is 205μm).

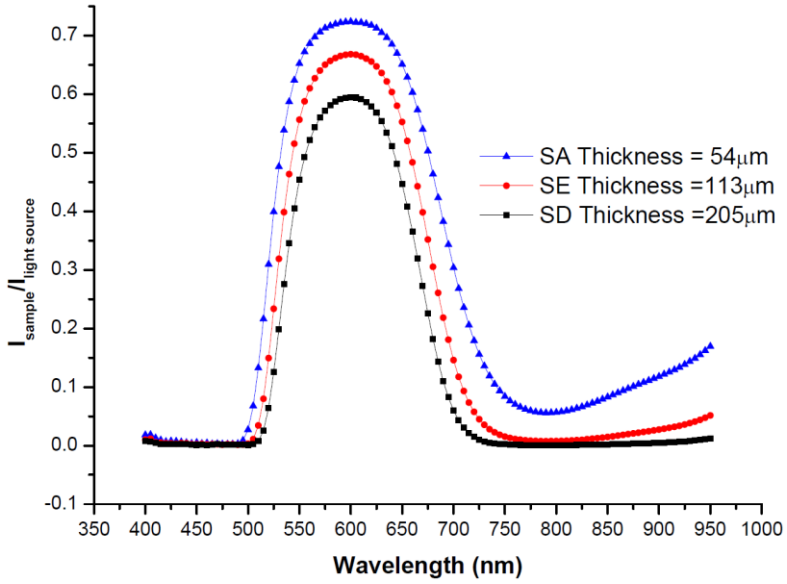

Figure 2 - Transmission of different samples with different thickness that is normalized to the light source spectrum (no sample) that shows the thinnest sample has transmitted the nearly 75% of light at 600nm.

Increasing temperature can affect the transmission due to structure changes induced by temperature increasing in the crystal. Figure 1 shows by increasing the temperature, the light transmittance reduces. Figure 3 shows reduction of transmission for few wavelengths. The reduction has linear relation with temperature lower than 344K and higher than 346K. This

reduction occurs due to varying distorted $CuCl_4$ octahedral structure. But there is an abrupt reduction between 344 and 346K that is related to the phase transition of the matter and we will discuss it later in detail.

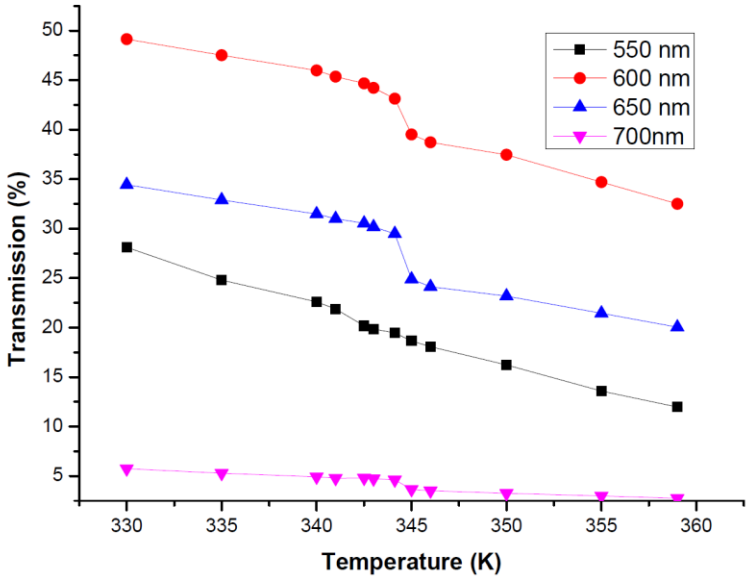

Figure 3- Transmission of sample versus temperature.

3.3.2 Birefringence vs Wavelength

As we derived in the previous section, to calculate the birefringence we need to measure the V_{1f} and V_{2f} (PEM modulated Signals) that are divided by DC signal. We will use the birefringence as an order parameter to study the phase transitions in Cu-Hybrid. When a material bears a phase transitions its structural variations can change its optical properties like absorption, reflectance, and transmission. Structural phase transitions (isotropic to anisotropic or vice versa, and also from one anisotropic to another anisotropic structure) under different physical conditions can be revealed by measurement their birefringence. Figure 4 shows the that V_{1f}/V_{DC} linearly decreases respect to the light wavelength and shifts to negative values by increasing the temperature. Around 343K, the behavior of V_{1f}/V_{DC} versus wavelength changes abruptly. After 343K it starts to shift up and the trend of the V_{1f}/V_{DC} with wavelength changes remarkably. The same procedure happens for V_{2f}/V_{DC} as shown in Figure 4.

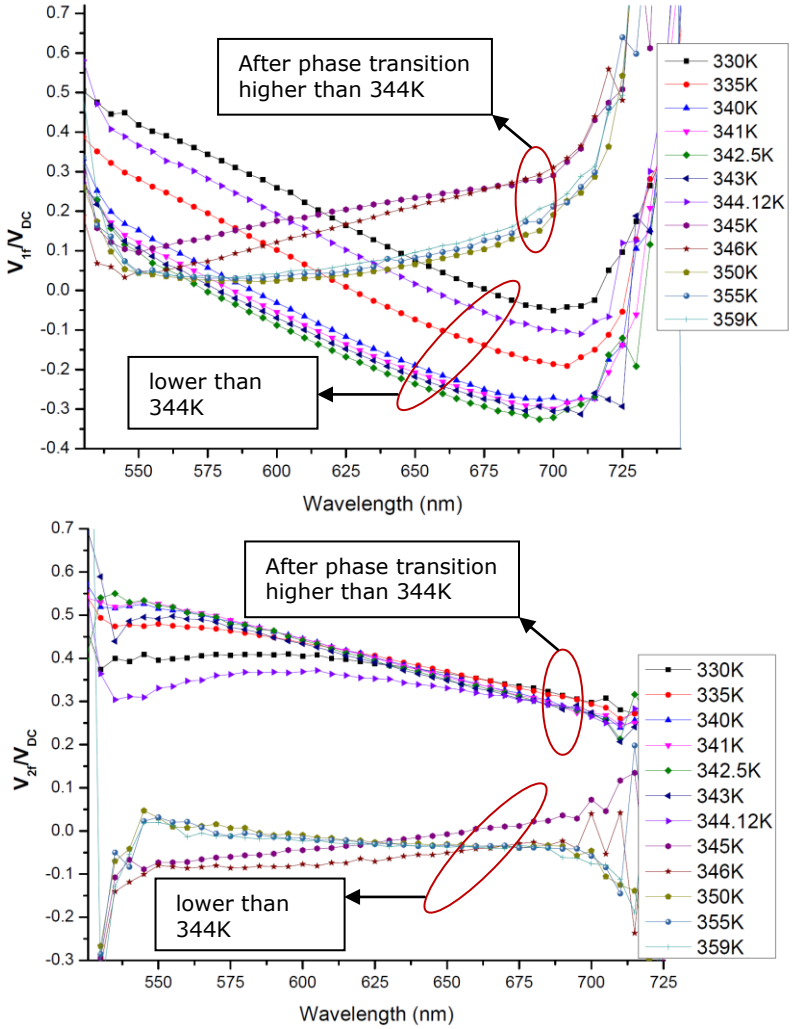

Figure 4- V_{1f} and V_{2f} signals that are divided by VDC signal at each temperature at Figure 1.

Now we are able to calculate the birefringence value of the sample, Δn. To calculate it, we used the equation 10 from previous section. From the figure we observe, Δn by increasing the value of temperature shifts to negative values but the situation is changed after 343K as explained for Figure 4. The other thing that seems interesting to discuss is the K value that we defined as dichroic parameter in the previous section. We cannot derive the a/b ratio from these graphs but instead we can calculate K that is equal to $2ab/(a^2+b^2)$. Anyway, K represents the dichroicity of the sample. It shows at high temperatures and also higher wavelengths, Cu-Hybrid finds much dichroic character. In other word, the sample is much dichroic at higher temperatures and wavelengths. As it can be seen from Figure 5, the situation is vice versa after phase transition, but sample is strongly dichroic.

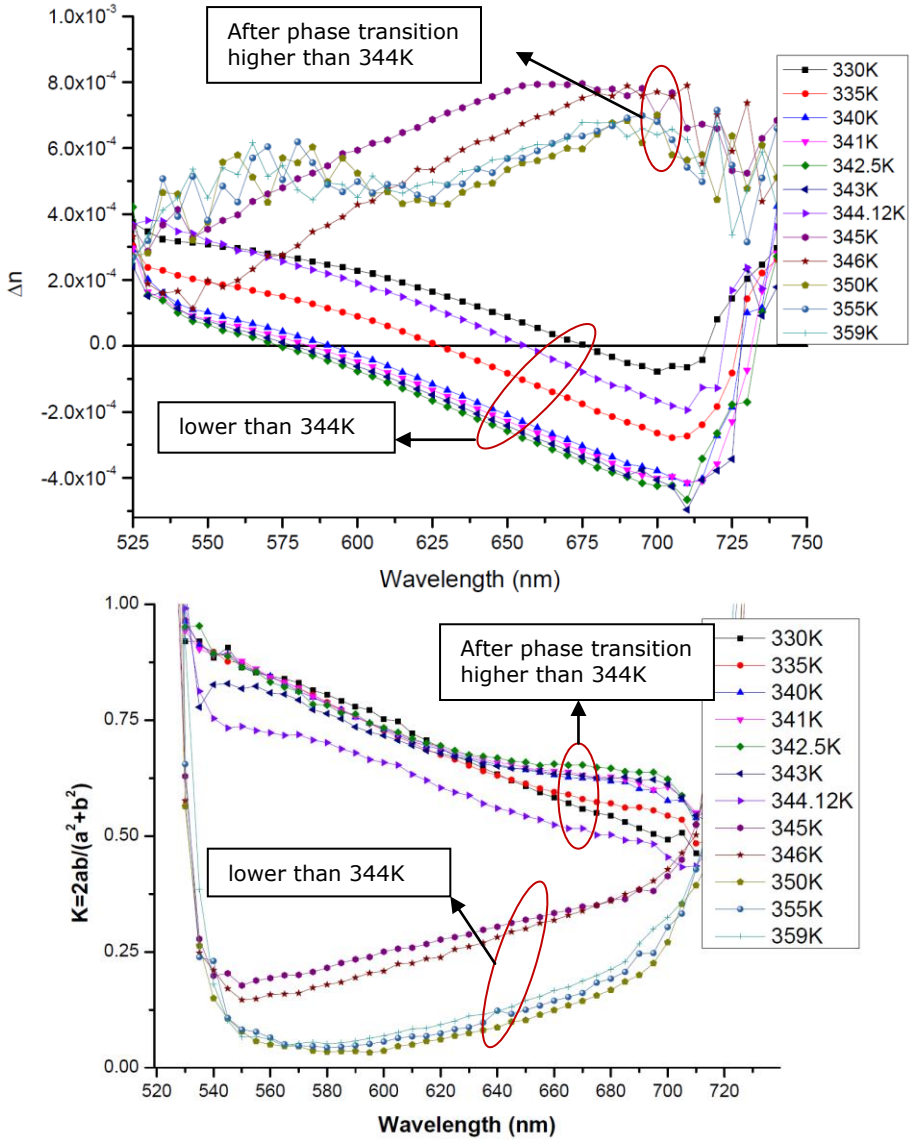

Figure 5- (up) Linear birefringence versus wavelength that is derived for different temperatures**, (down)** K value, that represents dichroic behavior of the sample.

To see better the birefringence behavior with temperature for different wavelengths, Figure 6 was extracted from Figure 5. It clearly shows after phase transition, Δn variation is much more pronounced for higher wavelengths. To probe temperature evolution of the birefringence, red light with wavelength 650nm have been chosen. At this wavelength, sample has the maximum transmission and is more reliable to measure the signals.

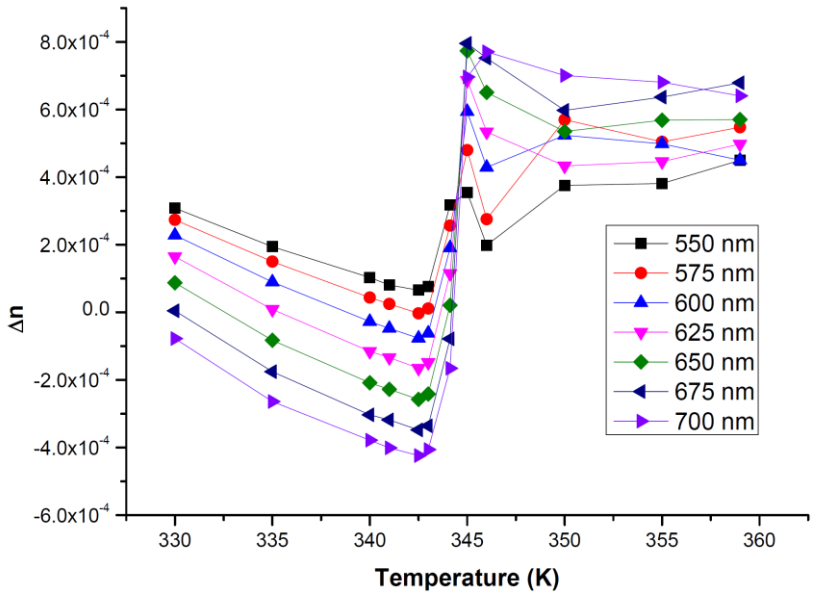

Figure 6- Birefringence evolution with temperature for different wavelengths.

3.3.3 Birefringence vs Temperature

To observe what happens when the temperature goes up, we measured birefringence temperature dependency from nearly 260 to 360K at wavelength 650nm. Cu-hybrid sample with thickness 205µm was probed and the data in Figure 7a were collected. All V_{DC}, V_{1f}, and V_{2f} signals show the phase change temperatures upon heating and cooling procedure. Around 344 the signature of the signals changes remarkably. Sample heating rate was 0.1 K/min. Upon cooling, the signals do not match exactly on the trace of heating signals, and they make a hysteresis loop from 340 to 356K. This behavior is shown in Figure 7b explicitly, that shows the sample birefringence behavior change with temperature. This plot shows a hysteresis loop at phase transition temperature that is the sign of first order phase transition.

$CuCl_4(CH_3CH_2NH_3)_2$ that is investigated extensively by different people, shows phase transition at 364K [12]. They have shown the mentioned hybrid and similarly hybrids like $CuCl_4(CH_3NH_3)_2$ (348K) and $CuCl_4(CH_3CH_2\ CH_2NH_3)_2$ (436) above the phase transition temperature are optically isotropic, and were assumed to be tetragonal (disordered but undistorted, in the high temperature phase) [12]. But our sample, PhC2Cu, behaves differently. It has relatively constant birefringence value from 80K to room temperature, but higher than room temperature it starts to decrease as shown in Figure 7b till it experiences the first order phase transition. It seems that high temperature phase is not optically isotropic and then its crystalline structure is not tetragonal. Our hybrid sample doesn't show fixed regular behavior in the high temperature phase and the repeating the measurement shows different amount of birefringence value at high temperature. It seems that $CuCl_4(C_6H_5CH_3CH_2NH_3)_2$ hybrid, after phase transition to HT phase flips the light direction back and upon cooling the inverse procedure occurs. The only thing that we can say is that, the structure is not so stable. The

measurement of birefringence in ambient pressure nearly certifies this idea that we will discuss later. Although it does not show stable behavior, but is shows that the structure of the sample is polar still. That is in contrast with Arkenbout results [**Error! Bookmark not defined.**].

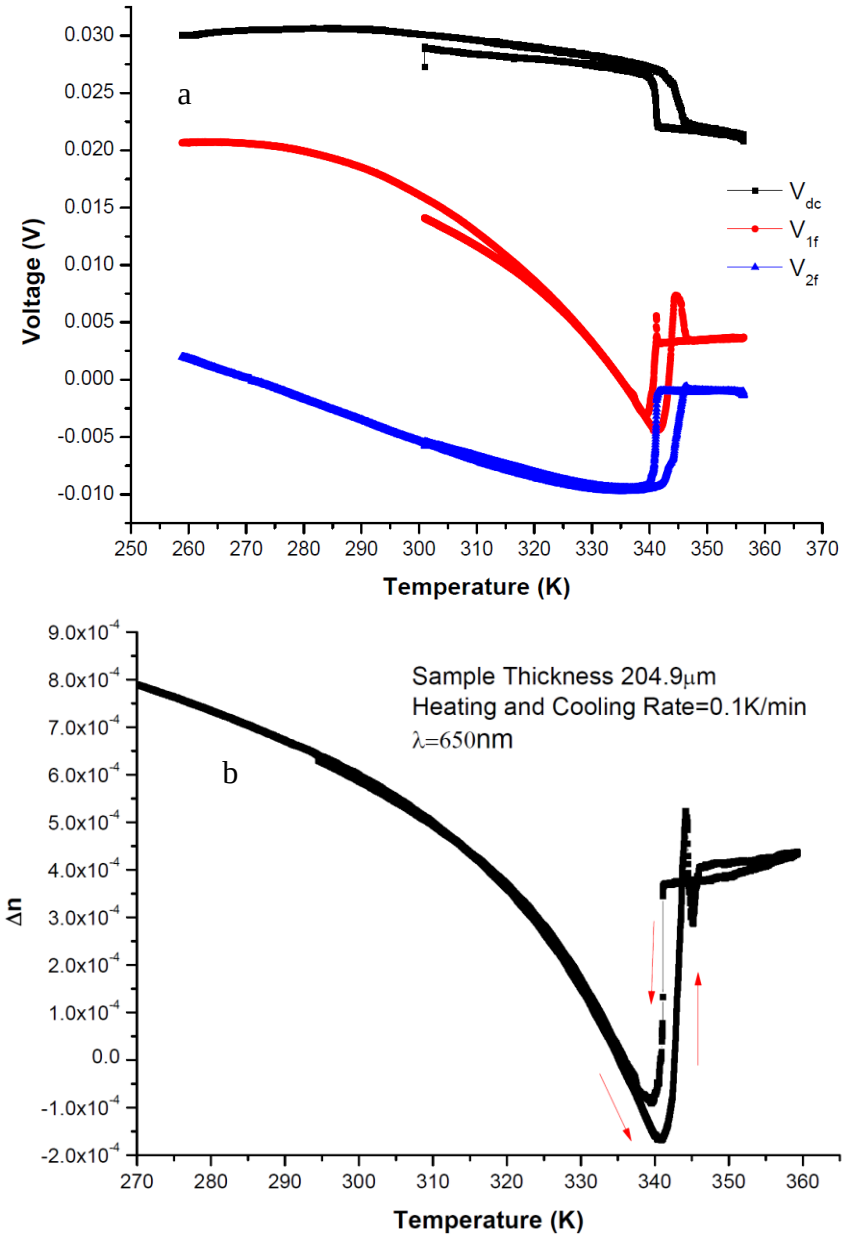

Figure 7- (a) V_{DC}, V_{1f}, and V_{2f} signals measured directly from set-up, (b) Birefringence of the Cu-Hybrid calculated from plot (a).

Figure 9 Shows the K value, that we introduced as a measure of dichroic behavior. The K value near to the room temperature and below is between 0.9-1 that means the sample is nearly non-dichroic. But with increasing the temperature of the sample, its dichroic character

increases and K value at 330K close to phase transition temperature shows a minimum. After phase transition Cu-Hybrid becomes extremely dichroic, that means in one of the directions absorption is much higher than the other axis.

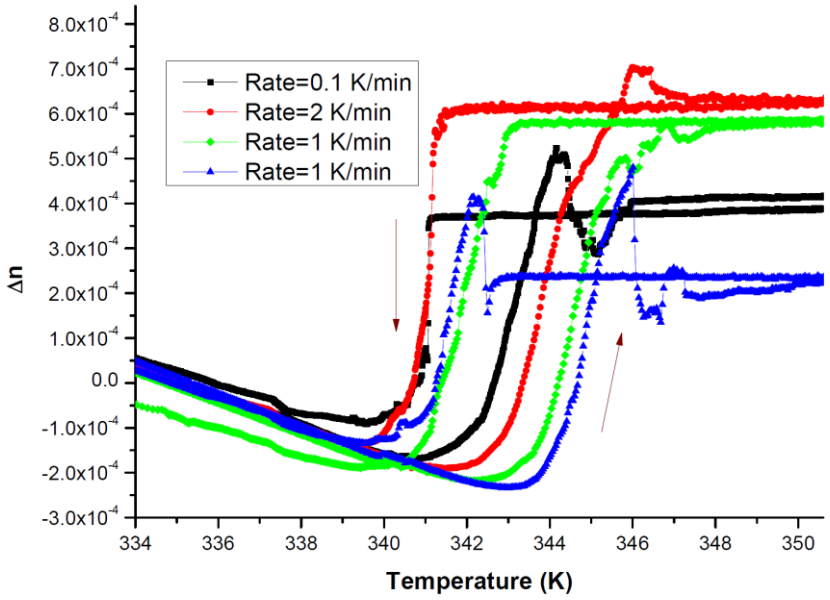

Figure 8- Different birefringent measurement at HT phase of PhC2Cu.

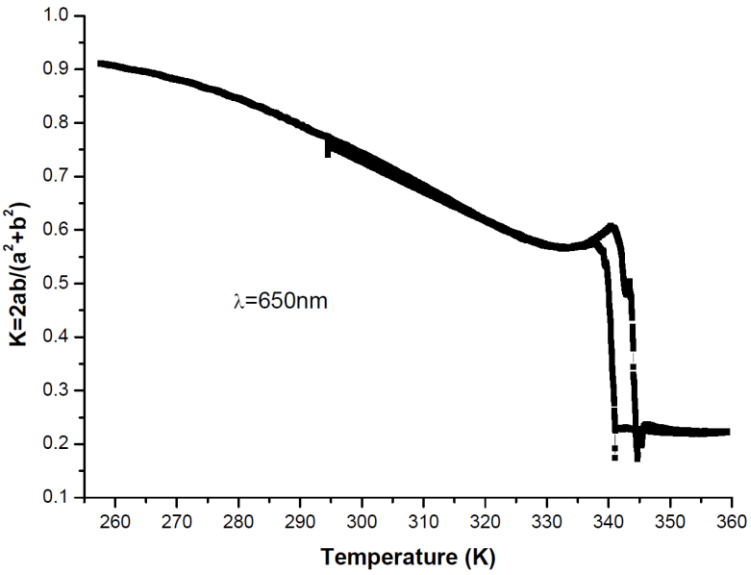

Figure 9- K value calculated using derived birefringence and V_{1f} signal, plot shows that the hybrid is nearly non-dichroic at room temperature and below, but strongly dichroic after phase transition.

3.3.4 Birefringence measurement at ambient Pressure

All the temperature dependent measurements that we presented till now were done inside the cryostat and vacuum medium. We did the same measurement at ambient pressure without

evacuating the cryostat. We observed that there is not remarkable difference with previous one (Figure 7) lower than phase transition Temperature The main differences that we observed were the sharpening of phase transitions and the birefringence rotated back in constant value (Figure 10). It seems that these effects are due to oxygen or water vapor. In our opinion, oxygen or water vapor sit on the hybrid molecules and don't let them to rebuild the structure that flips back the rotation.

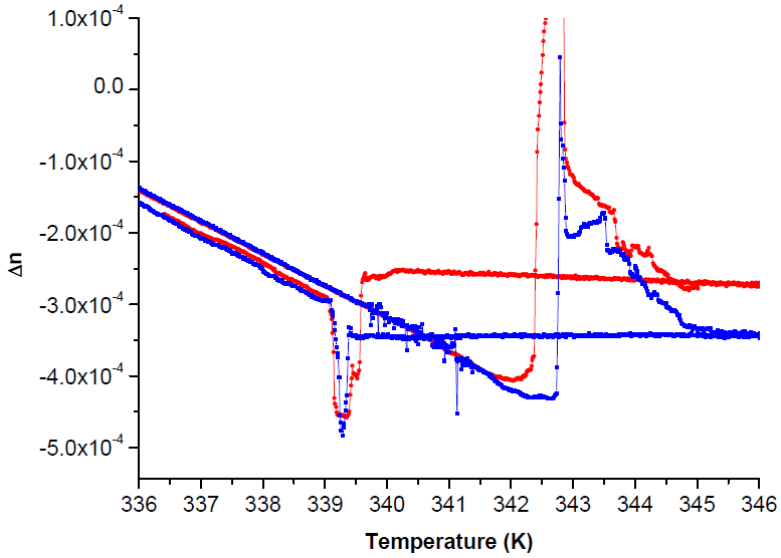

Figure 10- Birefringence measurement at room pressure.

3.3.5 Applied Electric Field Effect on Birefringence

In Cu-based hybrids $CuCl_4$ is a distorted octahedron that Cu2+ cations are in the middle of the octahedron. Due to this distortion, very small displacements of ammonium ions can induce a net polarization as discussed at chapter 1. Then it seems rational that by applying an electric field one can change the polarization direction. To do this we applied 300V DC voltage on the surface of the sample with distance approximately 1.5 mm, upon cooling down the sample. At first step we heated the sample up to high temperature and then we measured the birefringence dependence with temperature. In the next step while sample was cooling down we applied +300V on the sample. We did the same procedure with -300 volts. The results are shown in the Figure 11. This figure in comparison with the results that we considered shows very small difference around 336-340K. This difference can be seen well in the lower figure that is zoomed in on the mentioned interval. If we compare cooling curve that is poled and measured to unpoled measured one, we see a small deformation of +300V (upper) and -300V (lower) curves relative to not poled measured curves. Their behavior is opposite but different than un-poled measured curves.

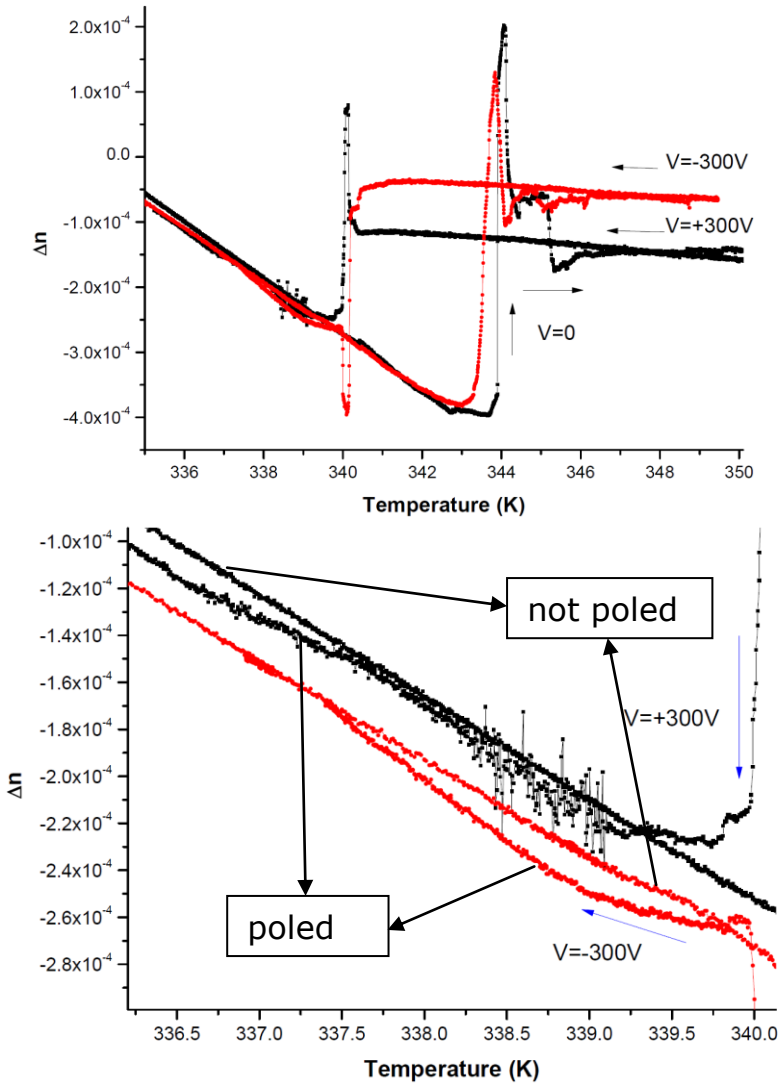

Figure 11- Applied electric field effect on birefringence change with temperature.

This measurement is repeated two times and the same results are observed that is shown in the Appendix B3. We believe if we measure the birefringence at higher applied electric field (~500V or higher) we will be able to see the polarization change effect at birefringence much pronounced.

3.4 Conclusion

We measured the birefringence behavior of Cu-Hybrid as an order parameter. Since Cu-Hybrid is a polar and optically anisotropic material, we employed this technique to study its phase transition behavior. Transmission spectra revealed, Cu-Hybrid absorbs the light below 500nm due to p-d transitions. Also we learnt that due to Jahn-Teller effect d-d transition was allowed for this compound.

The birefringence measurement revealed this matter at visible part is relatively non-dichroic but at higher wavelengths shows dichroic behavior.

Birefringence depends on temperature of the sample, because the structure of the sample changes slowly by increasing its temperature. This variation continues to nearly 344K and then its phase changes relatively suddenly. The phase change is a first order phase transition according to abrupt change and having a hysteresis phase transition loop. Evaluation of the samples dichroic behavior, showed Cu-Hybrid is strongly dichroic at higher temperatures. We investigated its temperature dependence at ambient pressure. This experiment showed the same phase transition behavior but with sharper structure transition relative to the experiments was done at vacuum condition.

All of birefringence measurements show that Cu-Hybrid is still polar after phase transition. These results are in contrast with Arkenbout results. So we need more X-Ray experiments to prove its structure at higher temperatures.

It is shown that poling the Cu-Hybrid can affect the structure of the sample and the orientation of the domains in it. The idea of poling it and make a uniform domains maybe is possible with higher voltages (>300K)

Acknowledgment

Living in Groningen had valuable experiences to me and I owe to many people due to that experiences. Now, it is going to finish my MSc. and I am going to thanks to all the people that I have learned and got helps, especially the people helped me in doing my master thesis.

During doing my master thesis work, I have had the chance of working in a group and sharing ideas. I have learned group work and how to do research in a group. This was exciting to me to see how the group members interact with each other and how they share their ideas, and discuss about the subjects all the time even at coffee breaks. They were helpful all the time and I would like to thank all of them at the first.

In the first semester, in spite of my back problem I did many experiments and most of the times it was really disappointing. But my supervisor Prof. Paul van Loosdrecht, was very patient with me and he tried to guide me in a proper way to learn scientific method of doing experiments with objectives that I am going to follow and answer the question. I hope I could be learnt to how to address my questions in my future works. Now, I want to sincerely thank my supervisor, Prof. Paul van Loosdrecht whose kind attentions led me through the difficulties. It was really instructing working under his supervision.

I appreciate Prof. Beariz Noheda for attending my master talk as a referee in spite of her tough schedule. She was my first supervisor in Groningen University and I have learned a lot from her.

Toni Caretta (PhD student in the OCMP) was who, maybe without his experiences and helps, I was not able to finish this work. He taught me how to work with Raman spectroscopy and analyze it. He also arranged with me the set of birefringence measurement that I measured my best results with that set-up. I would thanks for his great helps, especially helpful discussions that we had all the time during doing the experiments.

I gratefully acknowledge Foppe De Haan, andBen Hesp our group technical staffs that they were available for the help all the time.

Thanks to all group members, that I enjoyed being with you during coffee, lunch, and group meeting times with you and I am really happy to spend this period of my life with you.

I acknowledge the Zernike Institute for Advanced Materials, for giving scholarship and chance to study as a top-master in Groningen University.

At the end I would gratefully thanks to my mother and particularly my love who are always patient with me and encourage me to pursue exciting science.

4 Appendices

Appendix. A1

No.	Wavenumber cm-1	aa	ab	bb
1	17.5	T		T
2	20.5	T		T
3	61	W	S	W
4	66	T	T	W
5	70			T
6	72.5		T	T
7	75.5	W	T	W
8	80.7	W	T	
9	89.2		W	W
10	90.7		W	
11	93.7	T		
12	98.8	W	T	W
13	103			T
14	119	S	W	S
15	121		W	
16	126		W	
17	132	W	T	W
18	133.4		W	
19	136.3		W	T
20	141.5	W	W	W
21	144		W	
22	150.2		W	
23	151.34	W		W
24	154	W	T	W
25	161.2	T	S	W
26	167.7	W	S	W
27	176.1		T	
28	181.1		W	
29	189.5		T	T
30	209.6		W	S
31	225.1			T
32	235.8			W
33	239			W
34	247.5		T	T
35	272	T	T	S
36	338.4	T	T	T

Appendix. A2

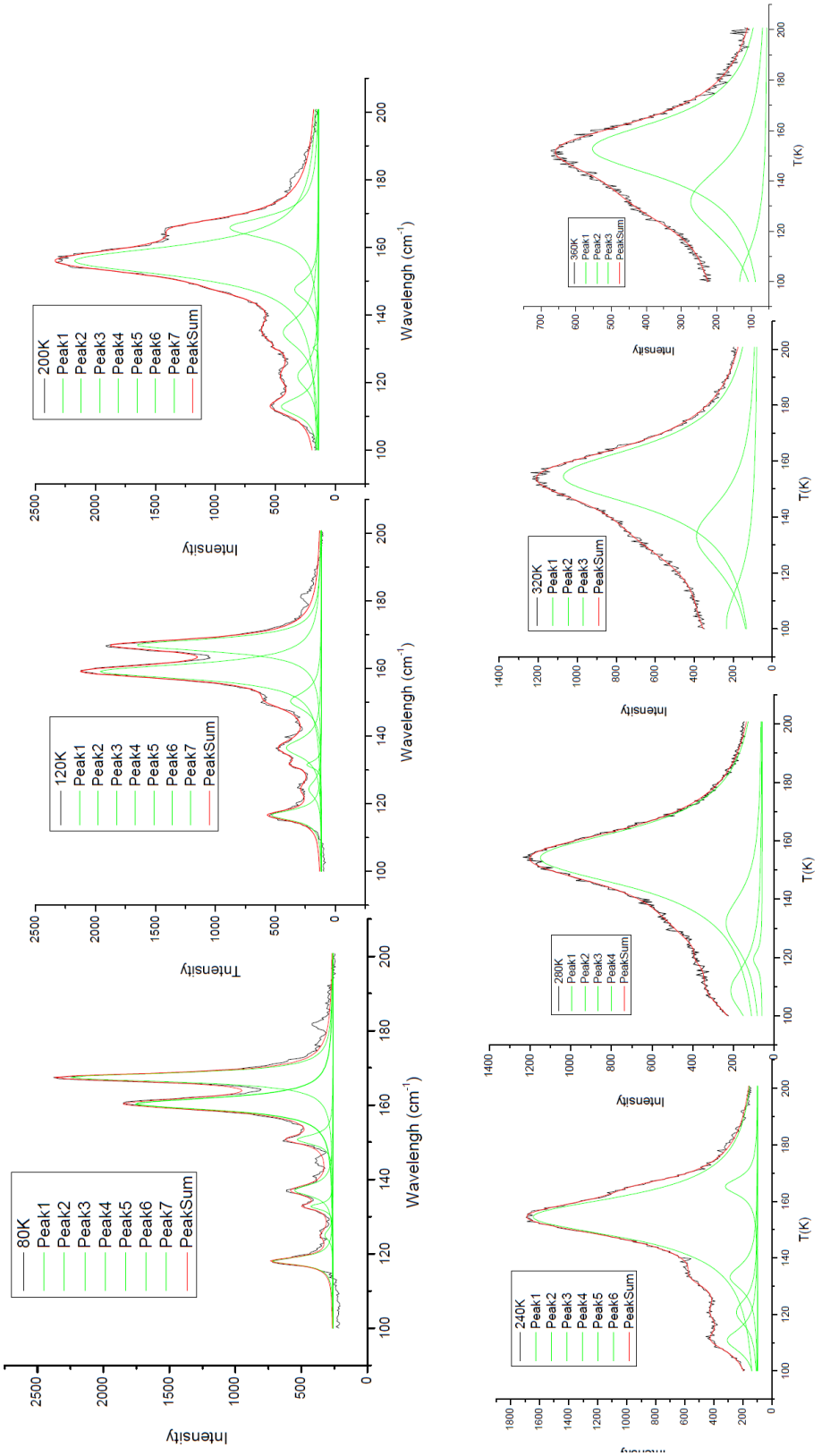
80K
120K
200K
240K
280K
320K
360K
Peak1
Peak2
Peak3
Peak4
Peak5
Peak6
Peak7
PeakSum
Intensity
Wavelengh (cm-1)
T(K)

Appendix B

Appendix B1- Set-up evaluation using Jones Matrices

Optical elements are described using 2 x 2 matrices that are called Jones matrices. These optical elements are polarizers (linear or right and left circular), phase retarders and so on. To see the effect of optical element, its matrix multiplied by polarized light vector. If we have a set of elements that light passes through, then the result is given by multiplication of elements matrices:

$$\begin{pmatrix} a_n & b_n \\ c_n & d_n \end{pmatrix}\cdots\begin{pmatrix} a_2 & b_2 \\ c_2 & d_2 \end{pmatrix}\begin{pmatrix} a_1 & b_1 \\ c_1 & d_1 \end{pmatrix}\begin{pmatrix} A \\ B \end{pmatrix}=\begin{pmatrix} A' \\ B' \end{pmatrix} \quad (5)$$

Using the proper matrix of each element (can be found in all general optic books and [13]), we can describe our system according to equation (5) as below according the set-up in Figure 2:

$$\begin{pmatrix} E_{xf} \\ E_{yf} \end{pmatrix}=\begin{pmatrix} 1 & 0 \\ 0 & 0 \end{pmatrix}R(-\theta)\begin{pmatrix} ae^{i\varphi_1} & 0 \\ 0 & be^{i\varphi_2} \end{pmatrix}R(\theta)R\left(-\frac{\pi}{4}\right)\begin{pmatrix} e^{i\delta(t)} & 0 \\ 0 & 1 \end{pmatrix}R\left(\frac{\pi}{4}\right)\begin{pmatrix} 0 & 0 \\ 0 & 1 \end{pmatrix}\begin{pmatrix} E_{xi} \\ E_{yi} \end{pmatrix} \quad (6)$$

where the R(θ) is the rotation matrix, the third matrix described the unknown sample (that is assumed is dichroic (a and b absorption coefficients 0<a,b<1) and birefringent (phase difference) at the same time. The matrix 6th from left describes the PEM,

$$R(\theta)=\begin{pmatrix} \cos(\theta) & \sin(\theta) \\ -\sin(\theta) & \cos(\theta) \end{pmatrix} \quad R(\theta)R(-\theta)=\begin{pmatrix} 1 & 0 \\ 0 & 1 \end{pmatrix} \quad (7)$$

If we take θ=π/4 then we will have:

$$I=E^*E=\frac{1}{4}{E_{yi}}^2(a^2+b^2-2ab\cos(\varphi_1-\varphi_2+\delta(t))),\ \ \delta(t)=A\cos(\Omega t)\ and\quad \varphi_1-\varphi_2=\Delta$$

$$\begin{aligned} I&=\frac{1}{4}{E_{yi}}^2(a^2+b^2-2ab\cos(\Delta+A\cos(\Omega t))) \\ &=\frac{1}{4}{E_{yi}}^2(a^2+b^2-2ab(\cos(\Delta)\cos(A\cos(\Omega t))-\sin(\Delta)\sin(A\cos(\Omega t)) \end{aligned} \quad (8)$$

We can expand the cosine of PEM oscillation amplitude as Bessel functions,

$$\cos(A\cos(\Omega t))=J_0(A)+2\sum_n^{\infty}(-1)^n J_{2n}(A)\cos(2n\Omega t)=J_0(A)-2J_2(A)\cos(2\Omega t)+\ldots \quad (9)$$

$$\sin(A\cos(\Omega t))=2\sum_{n=1}^{\infty}(-1)^{n+1}J_{2n-1}(A)\cos((2n-1)\Omega t)=2J_1(A)\cos(\Omega t)-2J_3(A)\cos(3\Omega t)+\ldots \quad (10)$$

By replacing equations 9 and 10 in equation 8 we can find 3 different intensities that is related to DC voltage that is the transmission of the sample. Two other signals are the modulated

signals from PEM that first is equal to 50kHz (PEM modulating signal or PEM vibration frequency) and the second 100kHz that is used to modulate the signal and get rid of other frequencies and noise making environment. Then we can write the intensities as a function of any frequencies that lock-ins modulate the signal.

$$I_0 = \frac{1}{4} {E_{yi}}^2 (a^2 + b^2 - 2ab\cos(\Delta) J_0(A)), \quad J_0(2.405) = 0, \; DC\,term \tag{11}$$

$$I_{1f} = abE_{yi}^{\;2} J_1(A)\sin(\Delta)\cos(\Omega t), \qquad 1f \tag{12}$$

$$I_{2f} = abE_{yi}^{\;2} J_2(A)\cos(\Delta)\cos(2\Omega t)), \qquad 2f \tag{13}$$

by choosing the amplitude of PEM equal to 2.405 then $J_0(A)$ will be zero and it will simplify the next calculations. Actually what we measure is the square root mean value of the above mentioned equations, by taking into account that

$$V_{DC} \propto I_0, \quad V_{1f} \propto I_{1f}, \quad V_{2f} \propto I_{2f}, \; V_{rms} = V/\sqrt{2}$$

we can derive the final equations as below that we will use to derive the birefringence of the hybrid crystals. By definition of K value as

$$K = \frac{2ab}{(a^2 + b^2)} \;\; if \;\; a = b \;\; then \;\; K = 1 \tag{14}$$

using square root value of equations 12 and 13 and dividing by DC signal value, we will have

$$\frac{V_{1f,rms}}{V_{DC}} = \sqrt{2} K \sin(\Delta) J_1(A) \tag{15}$$

$$\frac{V_{2f,rms}}{V_{DC}} = \sqrt{2} K \cos(\Delta) J_2(A) \tag{16}$$

By dividing equation 15 by equation 16, the birefringence equation can be derived that enables us to calculate birefringence. According to equation 3

$$\Delta = \arctan\left(\frac{J_2(A)}{J_1(A)} \times \frac{V_{1f,rms}}{V_{2f,rms}}\right) \Rightarrow n_1 - n_2 = \frac{\lambda\Delta}{2\pi d}\left\{\arctan\left(\frac{J_2(A)}{J_1(A)} \times \frac{V_{1f,rms}}{V_{2f,rms}}\right)\right\} \tag{17}$$

In the cases that crystal is non-dichroic, a and b coefficients are equal and the K coefficient in equation will be 1, and one can calculate birefringence just by measuring V_{1f} and V_{DC} (Equation 15).

According to definition of dichroism, a and b that are the absorption coefficients in different direction of uniaxial crystal, linear dichroism can be defined as the a/b. K value from equation

(14) can't give us the a/b, but we can use it to explain that the crystal is dichroic or not, if we know the birefringent value from equation 17.

Dichroic ratio (a/b) calculation

First Method

To derive a/b ratio, there is different strategies. First one can remove the analyzer (second polarizer close to detector) in the set-up and rotate the sample parallel to first polarizer (close to light source) (Figure 2). Jones calculation can be done as below for this system,

$$\begin{pmatrix} E_{xf} \\ E_{yf} \end{pmatrix} = \begin{pmatrix} ae^{i\Delta} & 0 \\ 0 & b \end{pmatrix} R\left(-\frac{\pi}{4}\right) \begin{pmatrix} e^{i\delta(t)} & 0 \\ 0 & 1 \end{pmatrix} R\left(\frac{\pi}{4}\right) \begin{pmatrix} 0 & 0 \\ 0 & 1 \end{pmatrix} \begin{pmatrix} E_{xi} \\ E_{yi} \end{pmatrix} = \frac{1}{2} \begin{pmatrix} ae^{i\Delta}(e^{i\delta(t)} - 1) \\ b(e^{i\delta(t)} + 1) \end{pmatrix}$$

$$I = \frac{1}{4} {E_{yi}}^2 (2a^2 + 2b^2 - 2(b^2 - a^2)\cos(A\cos(\Omega t)))$$

$$= \frac{1}{2} {E_{yi}}^2 \left\{ a^2 + b^2 - 2(b^2 - a^2)(J_0(A) - 2J_2(A)\cos(2\Omega t) + \ldots) \right\} \quad if \quad J_0(A) = 0$$

$$I_{DC} = \frac{1}{2} {E_{yi}}^2 (a^2 + b^2),$$

$$I_{2f} = 2{E_{yi}}^2 (b^2 - a^2) J_2(A)\cos(2\Omega t))$$

$$V_{DC} \propto \frac{1}{2} {E_{yi}}^2 (a^2 + b^2), \qquad \frac{V_{2f}}{V_{DC}} = 2\sqrt{2} J_2(A) \frac{b^2 - a^2}{b^2 + a^2}$$

$$V_{2f} \propto \sqrt{2} {E_{yi}}^2 (b^2 - a^2) J_2(A)$$

$$LD \propto \frac{V_{2f}}{V_{DC}} \qquad CD \propto \frac{V_{1f}}{V_{DC}}$$

Second Method

If in the general case matrix suppose the sample angle regarding to polarizer be 0 and 90 we will find:

$$I_0 = \frac{1}{2} {E_{yi}}^2 a^2 (1 - \cos(\delta)), \quad \theta = 0,$$

$$I_0 = \frac{1}{2} {E_{yi}}^2 b^2 (1 + \cos(\delta)), \quad \theta = 90$$

$$\frac{V_{DC}(\theta = 0)}{V_{DC}(\theta = 90)} = \left(\frac{a}{b}\right)^2$$

$$I_0 = \frac{1}{2} {E_{yi}}^2 a^2 (1 - \cos(\delta)) = \frac{1}{2} {E_{yi}}^2 a^2 (1 - J_0(A) + 2J_2(A)\cos(2\omega t)) \Rightarrow \frac{V_{2f}}{V_{DC}} = 0.61$$

Appendix B2

Thinner sample birefringence measurment

To verify the validity of the measurements that is shown already we did the same experiment with a thinner sample, 48μm. Figure shows the birefringent measurement of this sample. The overall signature of the T-dependence of birefringence is mostly same with the sample we showed above with thickness 205μm. This sample also scanned few times and showed that high temperature phase doesn't show stable behavior. But the other big difference is the value of Δn that is nearly 5 times greater that the thicker one as the thickness is

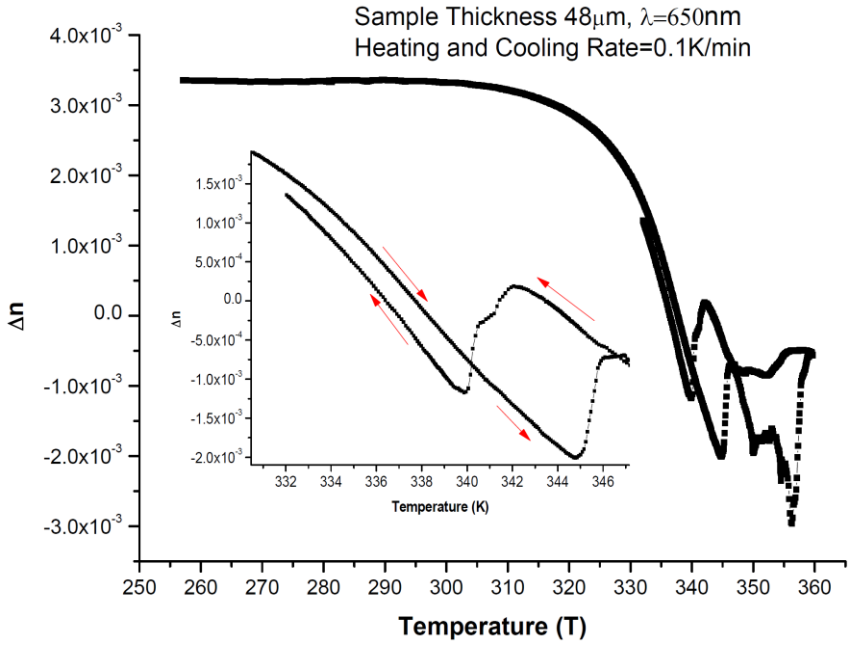

Birefringence behavior of PhC2Cu hybrid sample with thickness 48μm.

Appendix B3

Poling

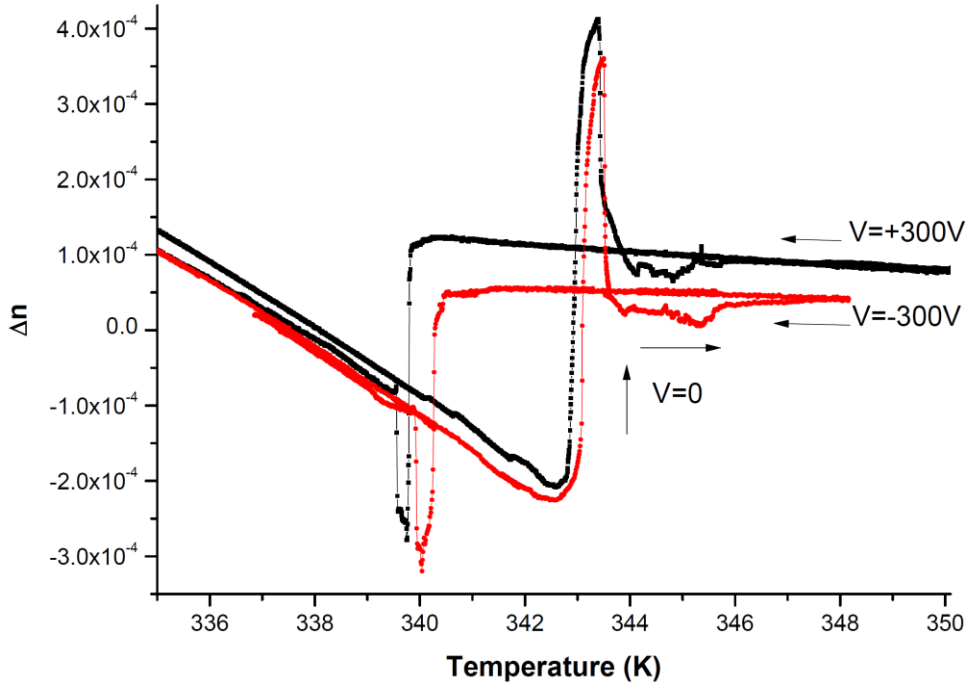

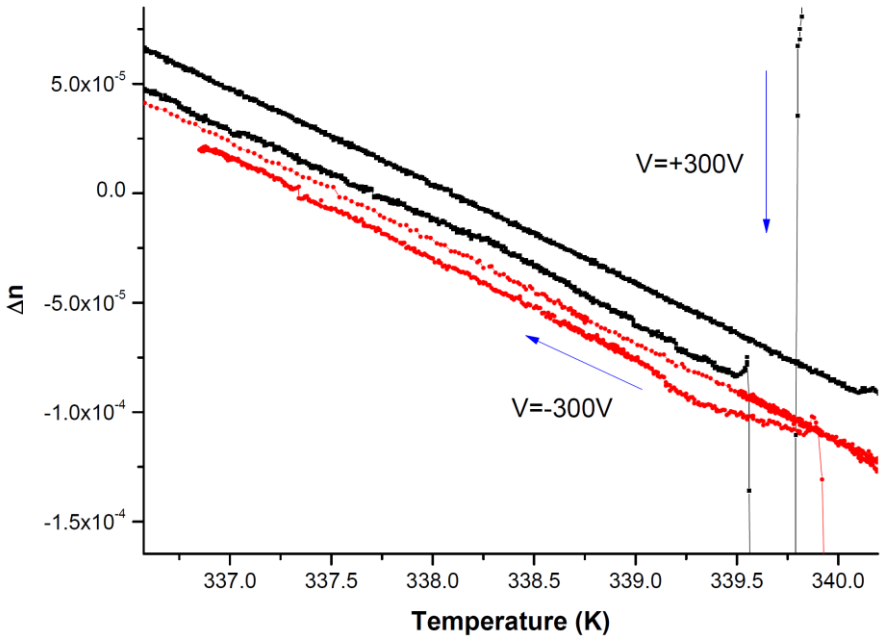

5 References

[1] C. N. R. Rao, A. K. Cheetham, A. Thirumurugan *"Hybrid organic-inorganic materials: a new family in condensed matter physics"* J. Phys. Condens. Matter **20,** 1 [083202] (2008).
[2] S. Blundell *"Magnetism in condensed matter"* Ch.4 1st ed. (2001) Oxford University Press, UK.
[3] .H. Kuzmany, "Solid State Spectroscopy", Springer, Berlin, 1998.
[4] N. Archiwa "Linear antiferromagnetic chains in hexagonal ABCl3-type compounds (A; Cs or Rb, B; Cu, Ni , Co, or Fe)" J. Phys. Soc. Jpn., 27, 561 (1969).
[5] V. J. Minkiewicz, D. E. Cox, G. Shirane "The magnetic structures of RbNiCl3 and CsNiCl3" Solid State Comm. 8, 1001 (1970) .
[6] D J Lockwood et al, " Raman Spectrum Of NiCl2", J, Phys. C: Solid State Phys., Vol.12, 1979
[7] D J Lockwood et al, "Raman Scatteringfrom the 1D antiferromagnets RbCoCl3 and RbNiCl3", J, Phys. C: Solid State Phys., 16 (1983).
8 http://en.wikipedia.org/wiki/Birefringence
9 http://www.star.le.ac.uk/~rw/courses/lect4313.html
10 Hecht, E. Opics, 2002
11 http://en.wikipedia.org/wiki/Jones_calculus
12 I R Jahn, et al, 1989 J. Phys.: Condens. Matter 1 6005
13 http://en.wikipedia.org/wiki/Jones_calculus